Journal of Neuroinflammation

RESEARCH

Open Access

Naïve Huntington's disease microglia mount a normal response to inflammatory stimuli but display a partially impaired development of innate immune tolerance that can be counteracted by ganglioside GM1

Noam Steinberg[1], Danny Galleguillos[1,2], Asifa Zaidi[1], Melanie Horkey and Simonetta Sipione[1*]

Abstract

Chronic activation and dysfunction of microglia have been implicated in the pathogenesis and progression of many neurodegenerative disorders, including Huntington's disease (HD). HD is a genetic condition caused by a mutation that affects the folding and function of huntingtin (HTT). Signs of microglia activation have been observed in HD patients even before the onset of symptoms. It is unclear, however, whether pro-inflammatory microglia activation in HD results from cell-autonomous expression of mutant HTT, is the response of microglia to a diseased brain environment, or both. In this study, we used primary microglia isolated from HD knock-in (Q140) and wild-type (Q7) mice to investigate their response to inflammatory conditions in vitro in the absence of confounding effects arising from brain pathology. We show that naïve Q140 microglia do not undergo spontaneous pro-inflammatory activation and respond to inflammatory triggers, including stimulation of TLR4 and TLR2 and exposure to necrotic cells, with similar kinetics of pro-inflammatory gene expression as wild-type microglia. Upon termination of the inflammatory insult, the transcription of pro-inflammatory cytokines is tapered off in Q140 and wild-type microglia with similar kinetics. However, the ability of Q140 microglia to develop tolerance in response to repeated inflammatory stimulations is partially impaired in vitro and in vivo, potentially contributing to the establishment of chronic neuroinflammation in HD. We further show that ganglioside GM1, a glycosphingolipid with anti-inflammatory effects on wild-type microglia, not only decreases the production of pro-inflammatory cytokines and nitric oxide in activated Q140 microglia, but also dramatically dampen microglia response to re-stimulation with LPS in an experimental model of tolerance. These effects are independent from the expression of interleukin 1 receptor associated kinase 3 (Irak-3), a strong modulator of LPS signaling involved in the development of innate immune tolerance and previously shown to be upregulated by immune cell treatment with gangliosides. Altogether, our data suggest that external triggers are required for HD microglia activation, but a cell-autonomous dysfunction that affects the ability of HD microglia to acquire tolerance might contribute to the establishment of neuroinflammation in HD. Administration of GM1 might be beneficial to attenuate chronic microglia activation and neuroinflammation.

*Correspondence:
Simonetta Sipione
ssipione@ualberta.ca
Full list of author information is available at the end of the article

Keywords Huntington's disease, Q140/140 knock-in mice, Ganglioside, Neuroinflammation, LPS, TLR4, TLR2, Tolerance, GM1, Microglia

Introduction

Huntington's disease (HD) is an autosomal dominantly inherited disorder characterized by neurodegeneration in the corpus striatum, in the cortex and other subcortical brain structures [1]. It results from the expansion (> 36) of a stretch of CAG trinucleotide repeats in the first exon of the gene that codes for huntingtin (HTT) [2–4]. This mutation translates into an expanded polyglutamine stretch that confers toxic properties to mutant HTT (mHTT) and induces its misfolding and aggregation [5–7].

HTT is ubiquitously expressed throughout the body, but it is particularly abundant in neurons and to a lesser extent in glial cells, including microglia [8–10], where, when mutated, it contributes to various aspects of disease pathology and progression [11–14]. Microglia are the myeloid cells of the brain and play a critical role in the normal development and homeostasis of the CNS [15–17]. Any alteration of the latter rapidly triggers microglia phenotypic variations according to the specific cues in the extracellular milieu [18–20]. Following detection of pathogens or tissue/cell damage, microglia acquire a pro-inflammatory phenotype that involves changes in gene expression and cell morphology, as well as secretion of pro-inflammatory cytokines such as IL-1β, IL-6 and TNF, among others [21]. The transient nature of this response is crucial to restoring homeostasis following tissue damage and repair. In many neurodegenerative conditions, however, microglia activation and the production of pro-inflammatory cytokines become chronic and contribute to disease onset and/or progression [22–24].

Pro-inflammatory activation of microglia is already detectable in pre-symptomatic HD patients [25–27], suggesting that it might be an early event in HD pathogenesis, and it correlates with disease progression at later disease stages [28]. Whether this pro-inflammatory state is induced by expression of mHTT in microglia in a cell-autonomous manner, by the response of microglia to the ongoing neurodegenerative process (even in prodromic HD), or both remains unclear. Studies in HD animal models have produced conflicting results, as microglia activation and neuroinflammation are present in some but not all models [29–42]. Furthermore, most studies have focused on the analysis of microglia morphology and density in vivo [31–40], or on the expression of inflammatory cytokines that are not exclusively produced by microglia [12, 31, 36, 38, 43], precluding the possibility to gain direct insights into the specific effects of mHTT expression in microglia.

In this study, we sought to shed light on the cell-autonomous phenotype of HD microglia in the absence of confounding effects from a diseased brain environment. We conducted an extensive analysis of the response of neonatal primary microglia isolated from Hdh140/140 (Q140/140) knock-in mice and wild-type (Q7/7) controls [44] in experimental paradigms that mimic microglia exposure to neurodegenerative conditions in vivo, including activation of the toll-like receptors (TLRs) 2 and 4 [45, 46] and exposure to necrotic cells [47, 48]. Our studies show that Q140/140 microglia respond to pro-inflammatory stimuli with similar kinetics and strength compared to wild-type microglia. However, Q140/140 microglia fail to develop full tolerance (i.e. to repress pro-inflammatory gene expression [49–51]) in response to repeated LPS stimulations, a dysfunction that could contribute to the establishment of chronic neuroinflammation [52]. Impaired or delayed tolerance was also observed in Q140/140 mice in vivo. We further show that treatment of Q140/140 microglia with ganglioside GM1, a glycosphingolipid with anti-inflammatory effects on activated wild-type microglia [53] and with disease-modifying effects in HD mouse models [36], dampens the production of pro-inflammatory cytokines in pre-activated Q140/140 microglia and strengthens tolerance in both wild-type and Q140/140 microglia.

Materials and methods

Animal and cells

Primary microglia cultures were prepared from homozygous Q140/Q140 knock-in mice expressing full-length mutant HTT with approximately 140 CAG repeats [54] and from wild-type Q7/Q7 mice [54]. Q140/Q140 mice were kindly donated by Cure HD Initiative (CHDI) and maintained on C57Bl/6J background in our animal facility. All procedures on mice were approved by the Alberta Animal Care and Use Committee and were in accordance with the guidelines of the Canadian Council on Animal Care. Neuroblastoma Neuro-2a (N2a) cells stably transfected with Exon1-mHTT97Q-eGFP or Exon1-wtHTT25Q-eGFP (hereafter referred to as N2a97Q and N2a25Q, respectively) were grown in DMEM (HyClone, SH30022.01): Opti-MEM (Gibco, 31985-070) (1:1) supplemented with 10% fetal bovine serum (FBS, Sigma

F1051), 1 mM sodium pyruvate (Gibco, 11360-070) and 2 mM L-glutamine (HyClone, SH30034.01).

Chemicals and reagents

Ganglioside GM1 purified from porcine brain was provided by TRB Chemedica Inc. (Switzerland) and resuspended in cell culture grade Dulbecco's phosphate buffered saline (DPBS, HyClone, SH30028.02). Lipopolysaccharide (LPS serotype O55:B5, gamma-irradiated) and lipoteichoic acid (LTA; from *Staphylococcus aureus*) were purchased from Sigma (L6529 and L2515, respectively). Recombinant mouse granulocyte–macrophage colony-stimulating factor (GM-CSF) was purchased from R&D systems (415ML/CF), recombinant human Interferon gamma1b (IFNγ1b) was purchased from Miltenyi Biotec (130-096-481). Exon1-mHTT97Q-eGFP and Exon1-wtHTT25Q-eGFP cloned in pcDNA3.1 plasmids were kindly provided by Dr. Janice Braun (University of Calgary).

Murine microglia cultures

Primary mixed glial cultures were prepared from P0.5-P1.5 Q140/140 and Q7/7 pups as described previously [55]. Briefly, after removal of the meninges, cerebral cortices were enzymatically and mechanically dissociated, and single cell suspensions were seeded in 12-well plates and cultured for 14 days in DMEM/F12 medium (Gibco, 11320-033) supplemented with 10% FBS, 100 U/ml penicillin – 100 µg/ml streptomycin (P/S, Hyclone, SV30010), 1 mM sodium pyruvate (Gibco, 11360-070) and 50 µM β-mercaptoethanol (Sigma, M3148). The cell medium was replaced every 4 days. On day 14–17, cultures were trypsinized as described [55], leaving adherent microglia attached to the bottom of the plate. Microglia were allowed to recover overnight in DMEM/F12 supplemented with 1 mM sodium pyruvate and 50 µM β-mercaptoethanol prior to experiments. Cells were maintained at 37 °C in 5% CO_2.

Functional studies

After isolation, microglia were cultured overnight in medium without FBS or P/S to let them recover. Microglia were then activated with or without LPS (100 ng/ml) or LTA (10 µg/ml) for the indicated time in fresh serum-free DMEM/F12 medium supplemented with 1 mM sodium pyruvate and 50 µM β-mercaptoethanol. For dose–response experiments with LPS, microglia were incubated with up to 1000 ng/ml LPS for 6 h. In experiments where the decay of the inflammatory response was measured, microglia were first treated with 100 ng/ml LPS for 12 h, then washed once with $HBSS^{+/+}$ (Gibco, 14025) containing 0.1% essential fatty acid-free bovine serum albumin (BSA; Sigma, A8806), once with $HBSS^{+/+}$ and twice more with DMEM/F12, and finally they were cultured in DMEM/F12 medium supplemented with 1 mM sodium pyruvate and 50 µM β-mercaptoethanol for 6–48 h to recover. In experiments that measured the development of tolerance, after stimulation with LPS and recovery in medium without LPS for 24 h as described above, cells were reactivated with 100 ng/ml LPS for 6 h. Microglia priming with GM-CSF and IFNγ was performed according to [56]. Briefly, one day after isolation, microglia were incubated in DMEM/F12 supplemented with 5% FBS, 1 mM sodium pyruvate, 50 µM β-mercaptoethanol and 5 ng/ml GM-CSF for 4–5 days, with a medium change after the first 48 h. Microglia were then primed for 1 h with 20 ng/ml IFNγ and activated with 100 ng/ml LPS for an additional 48 h. In all experiments where GM1 was used, after stimulation with the indicated factors, cells were washed once with $HBSS^{+/+}$ containing 0.1% essential fatty acid-free BSA, once with $HBSS^{+/+}$ and twice more with DMEM/F12 prior to incubation with 50 µM GM1 in DMEM/F12 supplemented with 1 mM sodium pyruvate and 50 µM β-mercaptoethanol. At the end of each experiment, the conditioned medium was collected for cytokine analysis and centrifuged for 2 min at 800×*g* at 4 °C to remove cellular debris. Cells were lysed in RLT plus buffer (QIAGEN) supplemented with β-mercaptoethanol (10 µl/ml) for RNA extraction, or in ice-cold 20 mM Tris pH 7.4, 1% IGEPAL® CA-630 (Sigma, I8896), 1 mM EDTA, 1 mM EGTA, 50 µM MG132 (EMD, 474790), 1×phosphatase inhibitor cocktail (PhosSTOP; Roche, 04906837001) and 1×protease inhibitor cocktail (cOmplete; Roche, 04693159001) for protein analysis. Protein concentration in cell lysates was measured with the bicinchoninic acid assay (Pierce).

Cell death assay

To measure cellular death, levels of lactate dehydrogenase (LDH) in the culture medium were quantified using CytoTox 96® cytotoxicity assay (Promega, G1780) according to the manufacturer's instructions. The absorbance at 490 nm was read in a SpectraMax i3x (Molecular Devices) and analyzed by SoftMax Pro 6.5.1 (Molecular Devices). Cytotoxicity was calculated as the percentage of total cellular LDH activity released in the conditioned medium. Cell death was also estimated by cell incubation with propidium iodide and high-content microscopy analysis. Briefly, cells were stained with 4 µg/ml Hoechst 33258 (Sigma, 861405) for 1 h and then incubated at room temperature with 2 µg/ml propidium iodide (Sigma, P4170) for 15 min prior to imaging with MetaXpress (Molecular Devices). Cell death was calculated from the percentage of Hoechst-positive cells that were also stained with propidium iodide.

Intraperitoneal administration of LPS in mice

Q7/7 and Q140/140 mice from both sexes were assigned to treatment groups based on their age and sex to ensure similar representation of both factors among the treatment groups. The mean mouse age was 7.8 months for Q7/7 mice (range: 5–11.2) and 8.3 months for Q140/140 mice (range: 3.5–11.2). Mice were injected intraperitoneally with saline or LPS in sterile saline solution at a daily dose of 0.5 mg per kg body weight, as previously described [51, 57, 58]. To induce inflammation, mice were administered saline for two consecutive days, followed by LPS injections for the last two days. To induce tolerance, mice received LPS injections for either 3 or 4 consecutive days (3×LPS or 4×LPS). Control animals received four saline injections. Three hours after the last injection, animals were anaesthetized using sodium pentobarbital and were transcardially perfused with ice-cold PBS through the left ventricle. The brain was removed and the cortex was dissected out and flash frozen in liquid nitrogen for protein analysis. Flash frozen tissues were homogenized in 50 mM TRIS, pH7.5, containing 150 mM NaCl, 1 mM EDTA and 1×phosphatase inhibitor cocktail (PhosSTOP; Roche) and 1×protease inhibitor cocktail (cOmplete; Roche). Linear regression analysis was performed to confirm that there was no correlation between mouse age and the response to LPS treatments or the development of tolerance for any of the cytokines measured.

Cytokines and nitrite quantification

TNF and IL-6 released in the microglia conditioned medium were quantified using mouse TNFα and IL-6 ELISA kits according to manufacturer's instructions (Invitrogen, 88-7324 and 88-7064-22, respectively) and a SpectraMax i3x spectrophotometer (Molecular Devices). Nitrite levels were measured by the Griess method using sulfanilamide (Sigma, S9251) and N-(1-Naphthyl) ethylenediamine dihydrochloride (Sigma, N9125), as previously described [59]. Cytokines in microglia conditioned medium and brain homogenates were analysed using a Luminex® multiplex assay (Thermo Fisher Scientific, Mouse High Sensitivity 18-Plex-MDHSTC18) by Eve Technologies Corporation (Calgary, AB, Canada). Cytokines and nitrite levels were normalized over the total protein content in the corresponding cell lysates or brain homogenates.

RNA extraction and qPCR analysis

Primary microglia were collected in RLT Plus buffer and total RNA was isolated and purified with the RNeasy Plus micro kit (QIAGEN, 74034) according to the manufacturer's instructions. mRNA was reversed transcribed using oligo dT primers (Invitrogen, 18418-012) and SuperScript II (Invitrogen, 18064-014). qPCR was carried out using PowerUp SYBR Green Master Mix (Applied Biosystems) in a StepOne Plus instrument (Applied Biosystems). Unless otherwise indicated, gene expression was normalized over the geometric mean of three reference genes encoding cyclophilin A, ATP synthase F1 subunit beta and Ribosomal Protein Lateral Stalk Subunit P0 (Normalization Index), according to [60].

Preparation of necrotic N2a cells

Necrotic cells were prepared from N2a25Q and N2a97Q cells. Cells were washed once with HBSS supplemented with 0.1% BSA and once with HBSS, trypsinized with 0.05% Trypsin/0.53 mM EDTA (Corning, 25051CI), spun down at 1,000×g and resuspended in DMEM/F12 medium supplemented with 1 mM sodium pyruvate and 50 µM β-mercaptoethanol at the concentration of 10^7 cells/ml. Five hundred µl of resuspended cells was transferred into a 15 ml tube and necrotic death was induced by applying 5 freezing–thawing cycles as previously described [61]. In each cycle, cells were incubated on dry ice for 2 min followed by thawing in a water bath at 37 °C for 2 min. The percentage of necrotic cells was assessed using trypan blue staining (HyClone, SV30084.01). Cells were exposed to the freeze–thaw cycle until > 98% cell death was achieved. Necrotic cells were immediately incubated with microglia for 4 h at a ratio of 2 necrotic cells per microglial cell.

Flow cytometry assay

To quantify plasma membrane TLR2 and TLR4 expression, microglia were detached from the culture dishes using StemPro Accutase (Gibco, A1110501), washed with cold HBSS and stained with LIVE/DEAD Fixable Far Red dye (Invitrogen, L34974) for 10 min on ice. Cells were then incubated with mouse FcR Blocking Reagent (Miltenyi Biotec, 130092575) for 10 min at 4°C, followed by incubation with 2 µg/ml PE/Cyanine7-conjugated anti-mouse TLR4 antibodies (BioLegend, 145407) or 2 µg/ml PE-conjugated anti-mouse TLR2 antibodies (BioLegend, 148603) for 30 min at 4 °C. Cells were then washed with 0.5% BSA and 2 mM EDTA in PBS, and fixed with 4% paraformaldehyde (Electron Microscopy Sciences, 15710) for 10 min. Samples were stored in 2% PFA at 4 °C prior to analysis using an Attune NxT Flow Cytometer (Invitrogen) in the Flow Cytometry Core Facility of the Faculty of Medicine & Dentistry at the University of Alberta. Data were analyzed using FlowJo software (version 10.7.1).

Statistical analysis

Two tailed *t*-test and ratio *t*-test analysis, Mann Whitney test, one-way ANOVA or two-way ANOVA with Tukey's, Sidak's or Dunnett's multiple comparisons test

were performed as indicated in the figure legends, using GraphPad Prism 9. A simple linear regression model was applied to confirm the lack of correlation between animal age and response to LPS in in vivo experiments, prior to pooling data from animals of different age. Paired estimation plots [62] of the effects of GM1 treatment on TNF secretion upon induction of tolerance were obtained using an online version of EstimationStats (https://www.estimationstats.com/#/). In each figure, N represents the number of independent experiments performed with different microglia cultures.

Results

Q7/7 and Q140/140 microglia respond with similar strength of activation to LPS stimulation

To determine whether HD microglia display cell-autonomous activation and/or exaggerated responses to inflammatory stimuli, we measured the expression of pro-inflammatory cytokines in primary microglia isolated from knock-in Q140/140 and Q7/7 mice, in naïve conditions and after stimulation with LPS, a TLR4 ligand. Naïve microglia of both genotypes had similar plasma membrane levels of TLR4 (Additional file 1: Fig. S1A.I) and did not express detectable levels of mRNA encoding pro-inflammatory cytokines, including IL-1β, IL-6 and TNF (Fig. 1A, B). Cell exposure to 100 ng/ml LPS induced upregulation of *Il-1b, Il-6* and *Tnf* mRNA expression (effect of time: $p < 0.05$), starting at 3 h of exposure, peaking at 9 h and then slowly decreasing at 24 h and 48 h of continuous LPS exposure (Fig. 1A). The gradual decrease in the transcription of pro-inflammatory genes after 9 h incubation in LPS was likely due to a physiological weakening of LPS-mediated signaling over time [63] and not to cell death, as there was no difference in cell survival between naïve and LPS-stimulated cells up to 24 h, and only a modest increase in the number of dead cells at 48 h compared to 24 h in Q7/7 microglia (effect of time: $p = 0.008$), but not in Q140/140 microglia (effect of time: $p = 0.21$) (Additional file 1: Fig. S2). The expression of pro-inflammatory cytokines over time and at each time-point was similar for Q7/7 and Q140/140 microglia, suggesting similar kinetics of TLR4 activation and downstream target gene transcription. Secretion of TNF (Fig. 1B) and nitric oxide (detected as nitrite in the conditioned medium, Fig. 1C) were also overall comparable between genotypes up to 48 h of incubation with LPS. At 6 h, the levels of TNF secreted by Q140/140 microglia appeared to be statistically different (and higher) compared to Q7/7 cells. However, considering that at later time points TNF secretion was comparable between genotypes and that mRNA expression was similar at all time points, the biological relevance of this statistical effect is likely negligible. These observations were further confirmed by the analysis of a broader panel of cytokines and proteins associated with inflammation, including TNF, IL1α, IL1β, IL2, IL4, IL5, IL6, IL7, IL10, IL12p70, IL13, IL17, MCP-1, LIX, MIP-2, KC, GM-CSF and INF-γ, using a highly sensitive Luminex® multiplex assay, which showed no differences in the overall response of Q140/140 and Q7/7 cells to LPS stimulation (Fig. 1D).

Next, we sought to determine whether Q140/140 microglia might be more sensitive than Q7/Q7 microglia to a milder stimulation, resulting in a stronger activation at lower doses of LPS. Expression of *Il-1b, Il-6* and *Tnf* (Fig. 1E*)*, and secretion of TNF into the medium (Fig. 1F) did not differ between Q7/7 and Q140/140 microglia at LPS concentrations ranging from 0.1 to 1000 ng/ml (Fig. 1E, F). Finally, we also observed no difference between the pro-inflammatory response of Q140/140 and Q7/7 microglia primed

(See figure on next page.)

Fig. 1 Comparable responses of Q7/7 and Q140/140 microglia stimulated with LPS. **A** Microglia were stimulated with LPS (100 ng/ml) for the indicated times. Expression of *Il-1b*, *Il-6* and *Tnf* mRNA at each time-point was normalized over the geometric mean of three housekeeping genes (Normalization Index). N ≥ 3. **B** TNF secreted in the conditioned medium was estimated by ELISA. N ≥ 3. **C** Nitrite in the conditioned medium. N = 8 for naïve microglia, N ≥ 4 for stimulated microglia. No statistically significant differences between genotypes were found for any of the measurements indicated above at any of the time points, except for TNF secretion at 6 h of LPS stimulation. **D** Proteins secreted in the conditioned medium after 9 h of cell treatment with 100 ng/ml LPS were quantified using a Luminex® multiplex assay. No statistically significant differences between genotypes were found for any of the cytokines and proteins measured. N = 5. **E**, **F** Dose–response of LPS stimulation. Microglia were stimulated for 6 h with LPS at the indicated concentrations and mRNA was quantified by qPCR. No differences in the expression of *Il-1b*, *Il-6* and *Tnf* mRNA (**E**), and the amount of TNF released in the medium (**F**) were observed between Q7/7 and Q140/140 microglia at all concentrations of LPS tested. N = 3 for Q7/7 and N = 4 for Q140/140 microglia. **G** Microglia were primed with GM-CSF for 4 days, followed by 1 h incubation in IFN-γ and 48 h in LPS to induce a pro-inflammatory state. Expression of *Tnf*, *Il-6* and *Il-10* was normalized as in (**A**). N ≥ 4. **H** mRNA expression of *Spi-1* was measured in control conditions and after stimulation for 12 h with LPS (100 ng/ml) and normalized as in (**A**). N ≥ 4. In **A**–**C** and **E**–**F**, a one-way ANOVA was used to confirm the effect of treatment in each genotype. The paired two-tailed *t*-test was used to compare differences between genotypes at each time point and LPS concentration. In **D**, two-tailed t-test was used to compare cytokine expression between genotypes. In **H**, a two-way ANOVA with Tukey's comparisons test was used. Bars are mean values ± STDEV. *, $p < 0.05$; **, $p < 0.01$

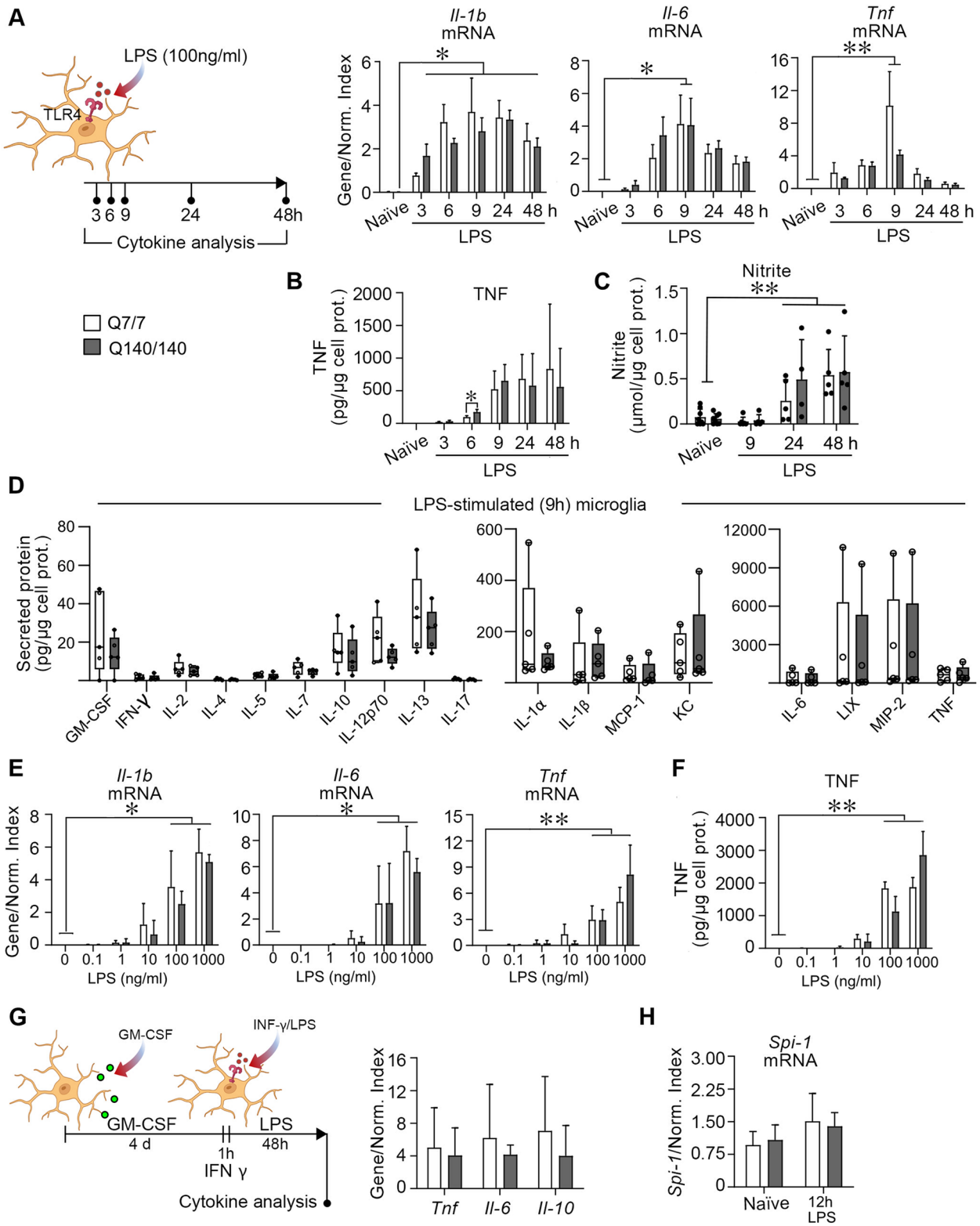

Fig. 1 (See legend on previous page.)

with GM-CSF for 4 days and with IFN-γ for 1 h prior to activation with LPS for 48 h, an alternative protocol commonly used to polarize microglia towards a pro-inflammatory state [56] (Fig. 1G).

It was previously suggested that expression of *Spi-1*, a key factor in myeloid fate determination, is upregulated in HD models and mediates cell-autonomous microglia activation and increased microglia response to LPS [12]. Consistent with their normal response to LPS stimulation and our previous in vivo studies [36], Q140/140 microglia expressed similar levels of *Spi-1* mRNA as Q7/7 microglia, in both naïve and stimulated conditions (Fig. 1H).

Q7/7 and Q140/140 microglia show comparable levels of activation following exposure to a TLR2 ligand or necrotic cells

Similar to TLR4, TLR2 is expressed in microglia [64] and contributes to microglia activation in neurodegenerative contexts [64–67]. Q7/7 and Q140/140 microglia express similar levels of TLR2 at the plasma membrane (Additional file 1: fig. S1B). To investigate the response of Q140/140 microglia to TLR2 stimulation compared to Q7/7 cells, we incubated microglia with lipoteichoic acid (LTA, 10 µg/ml), a TLR2 ligand [63] (Fig. 2A). This treatment resulted in upregulation of *Il-1b*, *Il-6* and *Tnf* transcription ($p < 0.05$, Fig. 2B) and secretion of TNF

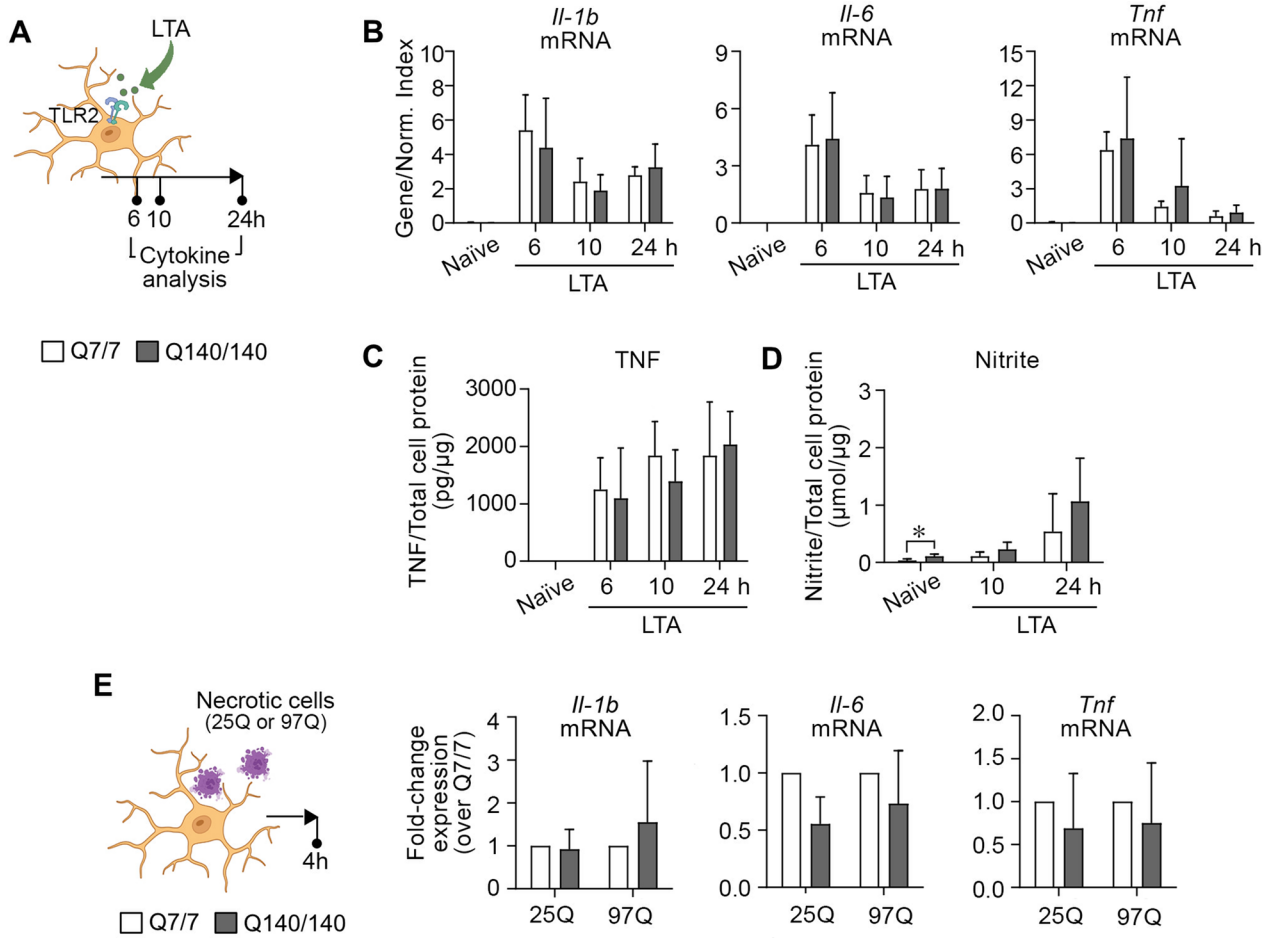

Fig. 2 Q7/7 and Q140/140 microglia display similar levels of activation in response to TLR2 ligands and necrotic cells. **A** Schematic experimental design showing the time points for cytokine analysis. Q7/7 and Q140/140 microglia stimulated with LTA (10 µg/ml) for 6, 10 and 24 h express similar levels of *Il-1b*, *Il-6* and *Tnf* mRNAs (**B**), and secrete similar amounts of TNF (**C**) and nitric oxide (**D**) in the medium. Gene expression was normalized over the geometric mean of three housekeeping genes (Normalization Index). One-way ANOVA was used to confirm an effect of treatment in each genotype. Unpaired two-tailed *t*-test was used to compare between genotypes at each time point. N ≥ 3. **E** Microglia were incubated with necrotic N2a cells expressing wild-type HTT exon 1(25Q) or mutant HTT exon 1 (97Q) at the ratio of 1:2 (microglia to necrotic cells). mRNA expression of *Il-1b*, *Il-6* and *Tnf* was measured after 4 h by qPCR. Graphs show fold change of mRNA expression in Q140/140 microglia compared to Q7/7 microglia exposed to the same type of necrotic cells. N ≥ 4. Ratio paired *t*-test was used to compare between the genotypes following activation with each specific type of necrotic cell. Bars are mean values ± STDEV. **p < 0.05*

($p < 0.05$) by cells of both genotypes to a similar extent (Fig. 2C). The levels of nitrite in the conditioned medium after stimulation with LTA were also similar between Q7/7 and Q140/140 microglia cultures (Fig. 2D).

To further mimic microglia exposure to activating conditions that are present in neurodegenerative diseases, we incubated microglia with necrotic N2a25Q and N2a97Q cells (Fig. 2E). This resulted in similar levels of activation in Q7/7 and Q140/140 microglia (as measured by the expression of pro-inflammatory cytokine mRNA). Interestingly, incubation of microglia with necrotic N2a97Q cells induced a higher expression of *Il-1b* and *Il-6* compared to exposure to necrotic N2a25Q (Additional file 1: Fig. S3).

Overall, our data suggest that Q7/7 and Q140/140 microglia respond in a similar manner and with similar kinetics to different types of pro-inflammatory stimuli that are directly relevant to neurodegenerative conditions.

Q7/7 and Q140/140 microglia display similar kinetics of deactivation after stimulation with LPS

The ability of microglia to cease a pro-inflammatory response when the initial activating stimulus is no longer present is crucial to tissue homeostasis and to prevent chronic microglia activation and tissue damage [52]. We exposed microglia to LPS (100 ng/ml) for 12 h and then monitored the time required for pro-inflammatory gene expression to return to baseline after the removal of LPS. Within 6 h from the end of LPS stimulation, expression of *Il1b, Il-6* and *Tnf* (Fig. 3A) and secretion of TNF (Fig. 3B) returned to baseline in microglia of both genotypes. To confirm this was due to TLR4 signaling waning off, rather than microglia cell death, we measure the latter at the end of LPS stimulation and 6 and 24 h post-stimulation. Microglia cell survival was not affected by the 12 h of LPS treatment, although slightly higher levels of lactate dehydrogenase (LDH) in the medium (a surrogate measure of cell death) were detected for Q140/140 microglia in both naïve and stimulated conditions compared to wild-type cells (effect of genotype: $F(1,8) = 5.82$, $p = 0.04$) (Additional file 1: Fig. S4, 12 h LPS). Cell death was minimal (below 10%) and similar in cells of both genotypes even at 24 h post-stimulation (effect of treatment: $(F1,8) = 5.68$, $p = 0.04$) (Additional file 1: Fig. S4), demonstrating that the waning of pro-inflammatory cytokine expression was not due to microglia cell death. Altogether, our data suggest that Q140/Q140 microglia have normal kinetics of deactivation upon cessation of the inflammatory stimulus.

Q140/140 microglia cannot develop full tolerance upon repeated LPS stimulation

Innate immune tolerance is a protective mechanism induced by a preconditioning stimulus that attenuates the inflammatory response to a second stimulation of similar nature [68], including LPS [49–51]. It is achieved by epigenetic modifications that silence the expression of pro-inflammatory cytokines and other potentially harmful genes following a first stimulation [69]. Similar to peripheral immune cells, microglia can acquire a tolerant state to prevent chronic activation and tissue damage [52, 70]. To investigate the ability of HD microglia to develop tolerance, microglia were first stimulated with LPS for 12 h, allowed to recover for 24 h, and then stimulated again with LPS for 6 h. Control cells were stimulated only once for 6 h (Fig. 4A). As expected, Q7/7 microglia developed tolerance and displayed an attenuated response to the second stimulation. This is clearly shown by the fold-change of pro-inflammatory cytokine expression

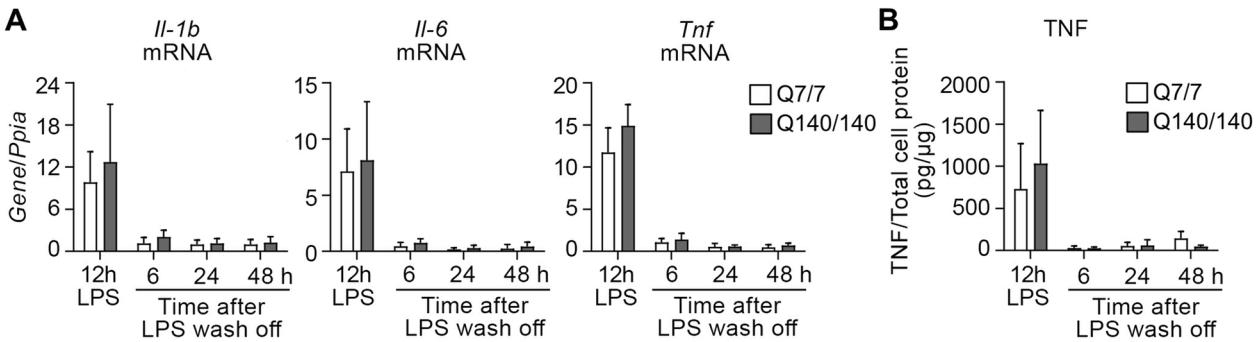

Fig. 3 Q7/7 and Q140/140 microglia display similar kinetics of recovery after LPS stimulation. Q7/7 and Q140/140 microglia were pre-incubated with LPS (100 ng/ml) for 12 h, washed and further incubated in serum-free medium for 6, 24 and 48 h. Expression of *Il-1b*, *Il-6* and *Tnf* (**A**, N ≥ 3) and levels of TNF secreted into the medium (**B**, N ≥ 4) were measured at the end of the incubation with LPS (12 h LPS) and during the recovery phase without LPS. mRNA levels were normalized over the housekeeping gene *Ppia* (encoding cyclophilin A). One-way ANOVA was used to confirm the effect of time on microglia phenotype of each genotype. An unpaired two-tail *t*-test was used to compare genotypes at each time-point. Bars are mean values ± STDEV. *$p < 0.05$, **$p < 0.01$, ****$p < 0.0001$

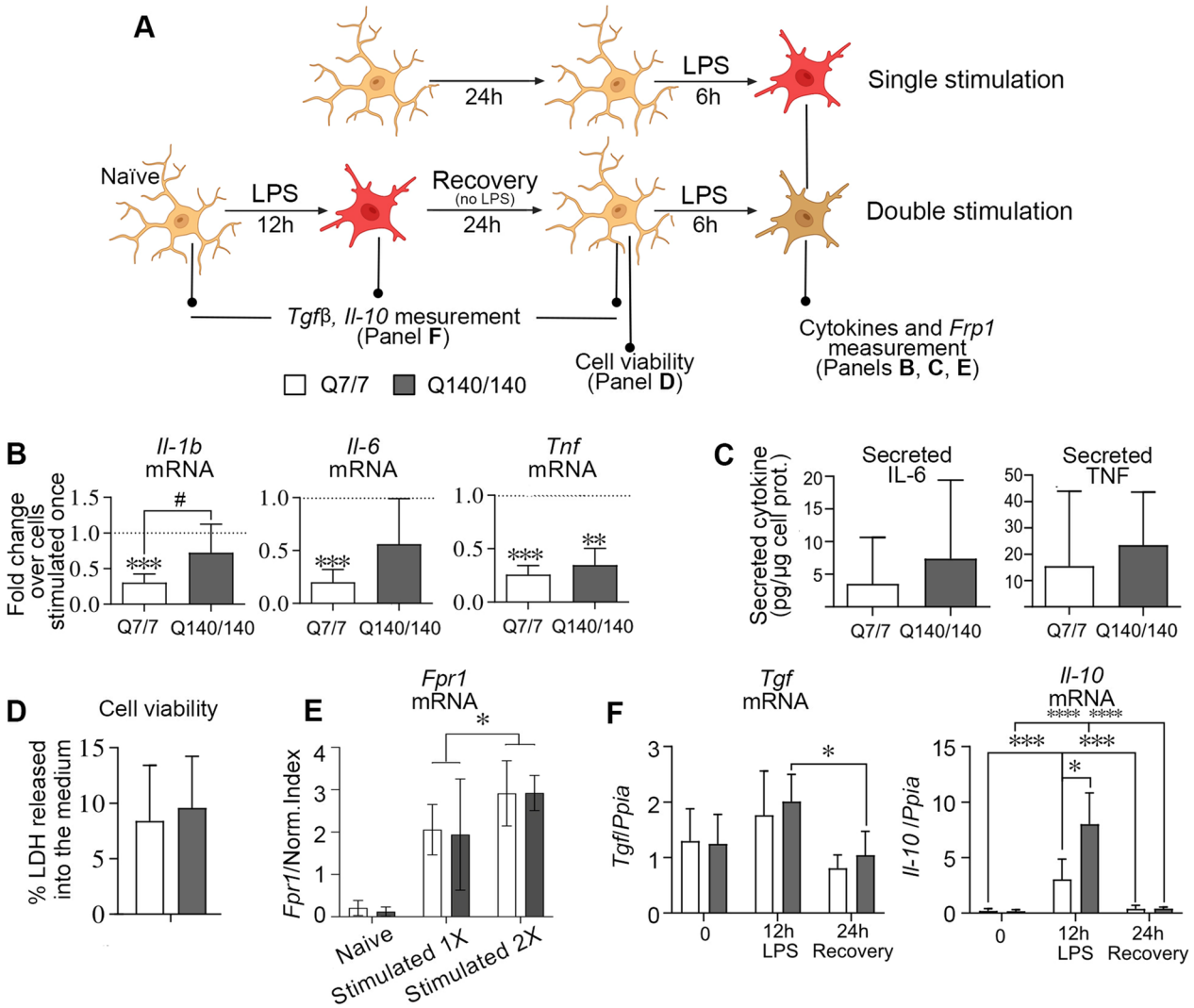

Fig. 4 Development of tolerance is partially impaired in Q140/Q140 microglia. **A** Schematic experimental design. Microglia were pre-treated with LPS (100 ng/ml) for 12 h, washed and incubated in serum free medium for an additional 24 h (recovery). A second stimulation with LPS (100 ng/ml) was performed for 6 h. Control groups were stimulated only once with LPS for 6 h. **B** Expression of *Il-1b*, *Il-6* and *Tnf* after the second stimulation with LPS is reported as fold-change compared to cells stimulated only once (baseline represented by the horizontal dotted line in each graph). mRNA levels were normalized over the geometric mean of three housekeeping genes. Ratio *t*-test. Asterisks show significant differences compared to the baseline of cells stimulated only once. The symbol # shows a statistically significant difference between genotypes. N ≥ 5. **C** Levels of IL-6 (N ≥ 4) and TNF (N ≥ 5) released by microglia in the culture medium. **D** Quantification of LDH released in the medium during 24 h recovery period following the first LPS stimulation. Similar levels of LDH released in the medium by Q7/7 and Q140/140 cells indicate microglia were healthy and had similar viability at the time of the second stimulation with LPS. Two-tailed paired *t*-test. N = 3. **E** Expression of the non-tolerizeable gene *Fpr1* is increased to a similar extent in Q7/7 and Q140/140 microglia stimulated for a second time with LPS, indicating gene priming. Two-way ANOVA and Sidak's multiple comparisons post-test. **F** *Il-10* and *Tgfb* mRNA expression in naïve microglia, at the end of the first stimulation with LPS and immediately prior exposure to the second dose of LPS (24 h recovery). mRNA levels were normalized over cyclophilin A levels. N ≥ 4 One-way ANOVA and Tukey's multiple comparison post-test were used to compare gene expression changes across time points for each genotype. Comparisons between genotypes at each time point were performed with the unpaired two-tail *t*-test. Bars are mean values ± STDEV. *$p < 0.05$, **$p < 0.01$, ***$p < 0.001$, ****$p < 0.0001$

(Fig. 4B) and secretion (Fig. 4C) relative to cells stimulated only once (dotted horizontal lines in Fig. 4B). In contrast, although *Tnf* expression and secretion (Fig. 4B, C) were attenuated in Q140/140 microglia after repeated LPS stimulation, *Il-1b* and *Il-6* expression were not significantly changed compared to the first stimulation (Fig. 4B), suggesting that these genes were not tolerized in Q140/140 microglia, at least not to the same extent as

in Q7/7 microglia. The mean levels of IL-6 secreted in the medium by Q140/140 microglia after the second LPS stimulation tended to be higher compared to Q7/7 cells (7.39 versus 3.55 pg/mg cell proteins, Fig. 4C), although the difference between genotypes did not reach statistical significance. Plasma membrane TLR4 levels (Additional file 1: Fig. S1A.III) and cell viability (Fig. 4D) were similar between Q7/7 and Q140/140 cells, confirming that impaired repression of *Il-1b* and *Il-6* gene expression in Q140/140 microglia was not due to reduced TLR4 signaling or decreased cell viability.

While pro-inflammatory genes are tolerized (i.e. repressed) in innate immune cells exposed to repeated stimulations with LPS, other TLR-induced genes involved in anti-microbial activities and tissue repair are not, and might even be primed for faster and increased expression to maintain optimal host defence and tissue homeostasis [69]. A prototypical gene that is primed after LPS stimulation is *Fpr1* (formyl peptide receptor 1) [69]. Expression of *Fpr1* was higher after the second stimulation with LPS in both Q7/7 and Q140/140 cells, with no significant differences between genotypes (Fig. 4E). Since priming of *Fpr1* depends on TLR4 activation and signaling as much as the silencing of pro-inflammatory genes, these data further confirm that the mechanism underlying impaired tolerance in Q140/140 microglia is downstream of TLR4 activation and is gene-specific.

IL-10 and TGF1β have been involved in the development of tolerance to LPS [71–73]. Therefore, we measured the expression of these cytokines after the first stimulation with LPS and during the cell recovery period to determine whether it could account for impaired tolerance in Q140/140 microglia. *Tgfb* expression was comparable between genotypes and not significantly increased after 12 h-stimulation with LPS (Fig. 4F). *Il-10* expression was transiently upregulated by LPS in cells of both genotypes, but to a greater extent in Q140/140 microglia compared to Q7/7 (Fig. 4F). Therefore, the impaired ability of Q140/140 microglia to develop full tolerance does not depend on a decreased expression of the tolerogenic cytokines TGFβ and IL-10.

Impaired or delayed development of tolerance in the brain of Q140/140 mice

Next, we sought to investigate tolerance in Q7/7 and Q140/140 mice in vivo. Previous studies have shown that intraperitoneal injection of LPS on two consecutive days induces inflammation in the brain and is followed by a state of tolerance characterized by reduced pro-inflammatory cytokine expression after subsequent LPS stimulation [51, 57, 58].

Using a similar experimental protocol (Fig. 5A), we confirmed that naïve Q7/7 and Q140/140 mice upregulate brain expression of pro-inflammatory cytokines and chemokines to similar levels when initially challenged with intraperitoneal LPS (Fig. 5B, 2X LPS). However, in tolerized mice (3X LPS) the levels of pro-inflammatory IL-1β, IL-6, TNF, IL-1α, IL-5, as well as the chemotactic molecules lipopolysaccharide-induced CXC chemokine (LIX) and the monocyte chemoattractant protein 1(MCP-1), remained significantly higher than in tolerized Q7/7 mice (Fig. 5B), requiring a fourth stimulation with LPS (4X LPS) to be lowered to Q7/7 levels. The only exceptions were GM-CSF and INF-γ, which were tolerized to a similar extent in both Q7/7 and Q140/140. Altogether, these data suggest that Q140/140 microglia in vivo are more resistant to tolerogenic stimulation than Q7/7 cells, since they need one additional stimulation to achieve the same level of suppression of pro-inflammatory gene expression as in Q7/7 microglia. As observed in our in vitro experiments, brain levels of IL-10 were not different between Q140/140 and Q7/7 mouse brains (Fig. 5B).

GM1 has anti-inflammatory effects on activated HD microglia and potently suppresses the expression of pro-inflammatory cytokines when administered prior to LPS re-stimulation

We previously showed that the administration of ganglioside GM1 exerts anti-inflammatory effects on normal microglia activated with various stimuli [53]. To determine whether GM1 would have similar effects on HD microglia and could be used to attenuate neuroinflammation in HD, we incubated Q140/140 microglia pre-activated with LPS with 50 μM GM1 for 6 h. GM1 decreased the expression of all pro-inflammatory cytokines by Q140/140 microglia (Fig. 6A), like in Q7/7 cells (Additional file 1: Fig. S5), and dramatically decreased the levels of nitrite in the conditioned medium of cells of both genotypes (Fig. 6B). Similar results were obtained when GM1 was administered to Q140/140 microglia primed with GM-CSF/INF-γ and then stimulated with LPS (Fig. 6C), or to microglia stimulated with LTA (Fig. 6D).

Next, we investigated whether treatment with GM1 could restore normal tolerance in Q140/140 microglia. Microglia treatment with the ganglioside during the recovery period (24 h) between the first and the second stimulation with LPS (Fig. 7A) resulted in an almost complete abolishment of pro-inflammatory cytokine expression and TNF secretion in both Q7/7 and Q140/140 cells (Fig. 7B, C). Expression of the non-tolerizeable gene *Fpr1* was also dramatically decreased compared to cells that were not pre-incubated with GM1 (Fig. 7D).

Incubation of peripheral monocytes with exogenous gangliosides was shown to cause upregulation of the interleukin-1 receptor associated kinase (IRAK)-M (also

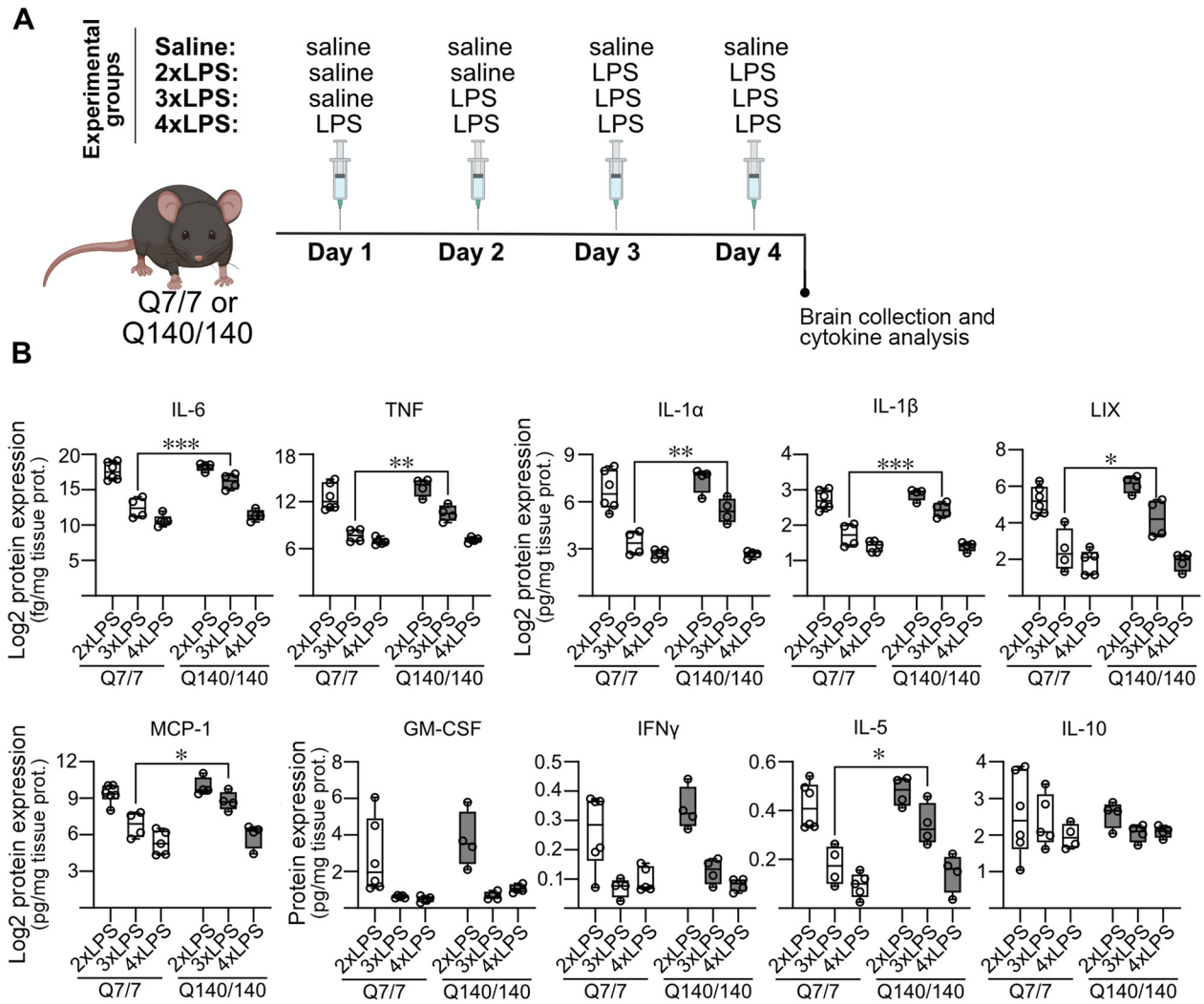

Fig. 5 In vivo development of tolerance is partially impaired or delayed in the brain of Q140/140 mice. **A** Schematic experimental design. Q7/7 and Q140/140 mice received daily intraperitoneal injections of saline or LPS (0.5 mg/kg) for 4 consecutive days, according to the indicated scheme. Two injections of LPS (2X LPS) on consecutive days were used to trigger inflammation in the brain. Three or four injections of LPS were performed to induce tolerance. **B** Cytokines in brain cortex homogenates were measured with a Luminex® multiplex assay. In tolerized (3X LPS) Q140/140 mice, the levels of several pro-inflammatory cytokines were significantly higher than in Q7/7 mice. A fourth LPS injection was needed to lower Q140/140 cytokine levels to Q7/7 levels. N ≥ 4. Two-way ANOVA with Sidak's multiple comparisons test. *, $p < 0.05$; **, $p < 0.01$; ***, $p < 0.001$

known as IRAK-3) [74], an established mediator of innate immune tolerance [75–77]. Therefore, we measured the expression of *Irak-3* to determine whether tolerance impairment in Q140/140 microglia and the dramatic effects of GM1 might be mediated by this protein. Expression of *Irak-3* was similar in tolerized Q7/7 and Q140/140 microglia (Fig. 7E) and, contrary to our expectations, it was dramatically decreased when cells were incubated with GM1 prior to a second stimulation with LPS (Fig. 7A, E). Naïve microglia treatment with GM1 did not affect the expression of *Irak-3* (Additional file 1: Fig. Fig. S6). Altogether, our data suggest that microglia pre-treatment with GM1 potently prevents microglia reactivation with LPS and dampens inflammatory responses with a mechanism that is independent of the expression of *Irak-3*.

Discussion

In this study, we sought to determine whether mHTT expression in HD microglia results in aberrant responses to inflammatory stimuli and abnormal microglia activation in a cell-autonomous manner. Previous work in HD mouse models has often produced inconsistent results. Increased microglia density and/

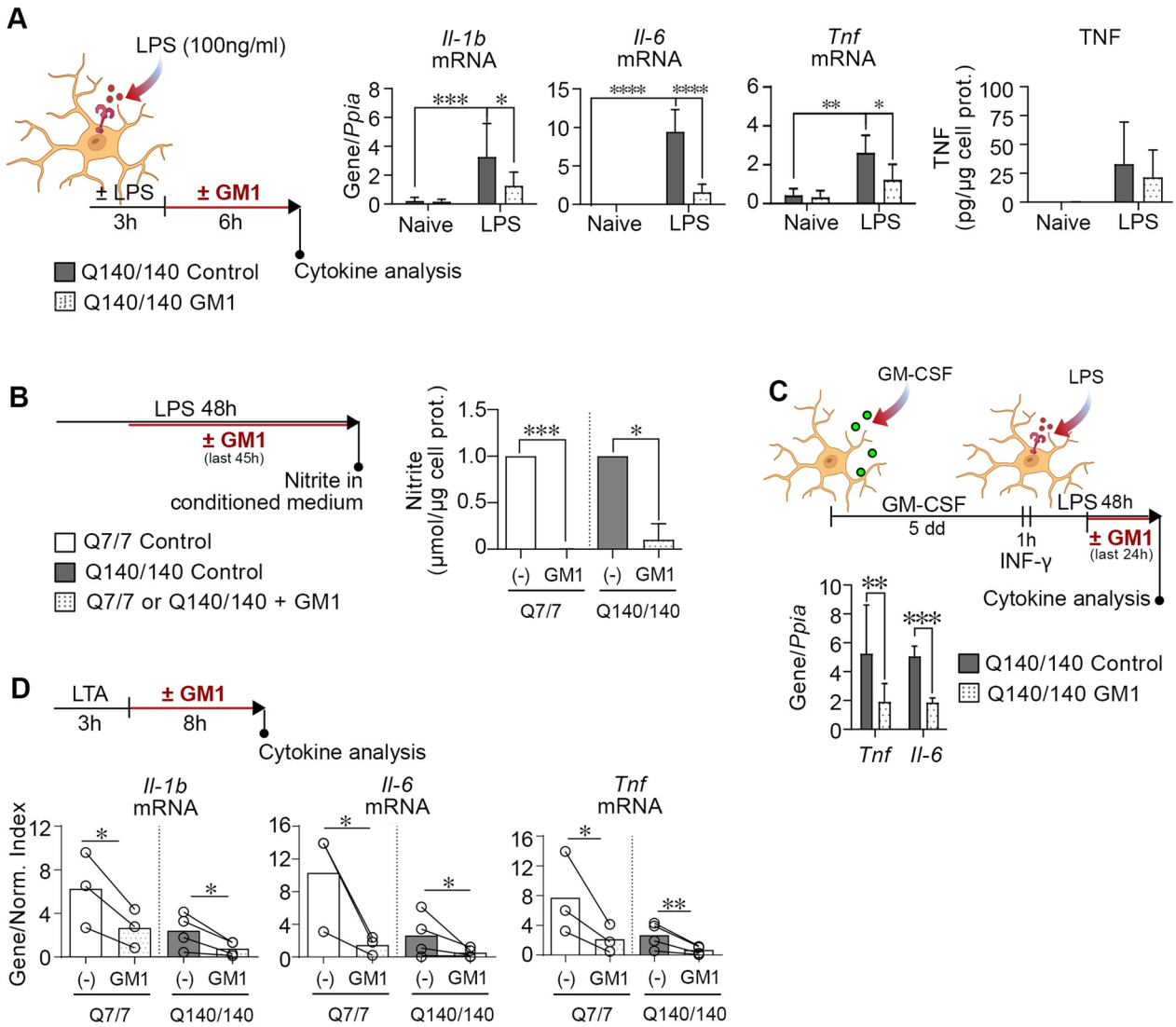

Fig. 6 GM1 dampens pro-inflammatory cytokines and NO production in Q140/140 and Q7/7 microglia. **A** Schematic experimental design and cytokine measurements. Q140/140 microglia were pre-treated with or without LPS (100 ng/ml) for 3 h, followed by washes and incubation with GM1 (50 µM) or vehicle (PBS) for 6 h. GM1 incubation significantly decreases the expression of *Il-1b*, *Il-6* and *Tnf* (N ≥ 4). Gene expression was normalized over the housekeeping gene *Ppia*. TNF secreted in the conditioned medium (N = 5) was normalized over the total cell protein content of the cells in each well. Two-way ANOVA with Tukey's multiple comparisons test. *$p < 0.05$, **$p < 0.01$, ***$p < 0.001$, ****$p < 0.0001$. **B** Microglia were treated with 100 ng/ml LPS for 3 h, followed by incubation with or without GM1 for 45 h. Levels of nitrite in the conditioned medium were normalized to total cell proteins. N ≥ 3. Two-way ANOVA with Sidak multiple comparison test. **C** Q140/140 microglia were polarized towards a pro-inflammatory phenotype by incubation with GM-CSF for 4 days, followed by 1 h priming with INF-γ and 48 h stimulation with LPS. GM1 or control vehicle were added for the last 24 h of incubation in LPS. Gene expression was normalized over *Ppia*. Ratio paired *t*-test. **D** Q7/7 and Q140/140 microglia were incubated with or without LTA (10 µg/ml) for 3 h, followed by washes and treatment with vehicle or GM1 (50 µM) for 8 h. GM1 significantly reduces the expression of *Il-1b*, *Il-6* and *Tnf* mRNA. Gene expression was normalized over the geometric mean of three housekeeping genes (Normalization Index). Ratio paired *t*-test. Bars are mean values ± STDEV. *$p < 0.05$, **$p < 0.01$, ***$p < 0.001$

or elevation of pro-inflammatory cytokines was shown in some studies [37–42] [12, 38, 42, 78, 79], but not in others [29–36], even when the same animal models were investigated. Inconsistencies across in vivo studies might not be surprising considering genetic differences and potential major confounding effects from environmental conditions and cell–cell interactions in the brain. Studies in isolated neonatal microglia from the same mouse models, however, have produced similarly inconsistent results, with some studies showing higher activation of microglia from R6/2 mice compared to wild-type microglia even in naive conditions

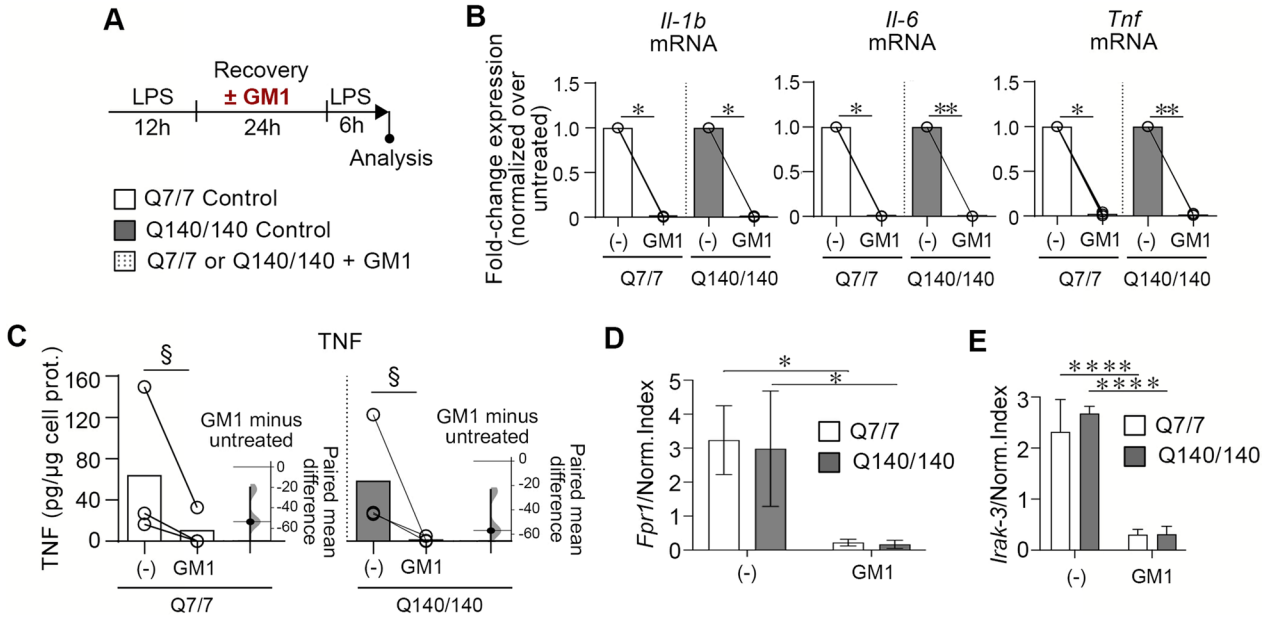

Fig. 7 GM1 dampens microglia reactivation in an experimental model of tolerance. **A** Experimental design. Microglia were stimulated with LPS (100 ng/ml) for 12 h, then washed and let recover in serum-free medium for 24 h in the presence or absence of GM1 (50 µM). After several washes to remove GM1, a second stimulation with LPS (100 ng/ml) was performed for 6 h, at the end of which, cytokine expression and secretion were measured. **B** Expression of *Il-1b, Il-6* and *Tnf* mRNA was normalized over the geometric mean of three housekeeping genes (Normalization Index). N = 3. Ratio paired *t*-test. **C** TNF secreted in medium. Data are presented as a paired estimation plot including individual data points (independent experiments), mean values shown by bars, and the bootstrap 95% confidence interval for the effect size. N = 3. §, $p = 0$ as per paired estimation plot. **D** *Fpr1* expression was measured in microglia stimulated twice with LPS as per experimental design in (**A**). GM1 presence during the recovery period represses the expression of the non-tolerizeable gene *Fpr1*. **E** Cells were treated as in (**A**). The expression of Irak-3 is similar in Q7/7 and Q140/140 cells. The presence of GM1 during the recovery period prevents upregulation of Irak-3 after re-stimulation with LPS. Two-way ANOVA with Sidak's multiple comparison post-test was conducted in **D** and **E**. Bars are mean values ± STDEV. *$p < 0.05$, **$p < 0.01$, ****$p < 0.0001$

[12, 78], and others showing higher activation only after microglia priming [43, 79].

In this study, we used microglia isolated from Q140/140 knock-in mice that express full-length mHTT from the endogenous mouse *Htt* gene locus, a model that closely resembles the genetic makeup of the human disease [44]. We demonstrated that Q140/140 microglia display kinetics of activation and deactivation in response to a range of pro-inflammatory stimuli that are remarkably like those in wild-type Q7/7 microglia. To mimic conditions that activate microglia in the context of neurodegenerative diseases, we exposed Q140/140 and Q7/7 microglia to ligands of TLR4 and TLR2, two pattern recognition receptors that can promote microglial-mediated neuronal injury and neurodegeneration [80, 81] upon stimulation by pathogenic misfolded proteins and/or endogenous danger-associated molecular patterns (DAMPs) released by injured and dying cells [66, 67, 82, 83]. In response to TLR4 and TLR2 stimulation, Q140/140 microglia upregulated the expression of pro-inflammatory genes such as *Il1-b, Il-6 and Tnf* and produced NO and TNF to a similar extent and similar kinetics as wild-type cells. Similar results were obtained when we screened for the secretion of a broader panel of cytokines using a highly sensitive Illumina platform. Our results are in contrast with a previous report where R6/2 microglia stimulated with LPS displayed higher activation compared to wild-type microglia [79]. Since the same concentration of LPS and a similar timeframe of stimulation were used in those experiments and in ours, the contrasting results might be due to differences in the genetic makeup of the models used (endogenous levels of expression of full-length mutant HTT in our studies *versus* transgenic expression of a more toxic mutant HTT-exon 1 fragment in R6/2 mice). In a different study, R6/2 microglia were shown to respond more strongly to LPS when primed with IFN-γ [43]. In our experiments, even when primed with IFN-γ Q140/140 microglia upregulated pro-inflammatory gene expression to the same extent as wild-type cells. The kinetics of microglia activation—i.e. the response to different doses of LPS and the time course of pro-inflammatory gene transcription and NO production—were similar between the two genotypes. Q140/140 microglia also retained a normal ability to taper off pro-inflammatory gene transcription upon removal of LPS.

To further mimic conditions that are present in a degenerating brain environment, Q140/140 microglia were incubated with N2a necrotic cells that expressed either wild-type or mutant HTT. Although neuronal death in HD and other neurodegenerative diseases predominantly occurs through pathways other than necrosis [48], stimulation with necrotic cells remains an established model to mimic microglia activation in neurodegenerative conditions where inflammatory intracellular components are released by cells [84–86]. Once again, Q140/140 and Q7/7 microglia reacted similarly to incubation with necrotic cells. Altogether, our experiments suggest that expression of full-length mutant HTT at physiological levels does not lead to cell-autonomous activation of murine microglia per se, nor to an exacerbated response to pro-inflammatory stimuli in naïve microglia. This is also supported by our in vivo data, which show that the levels of pro-inflammatory cytokines in the brain of Q7/7 and Q140/140 mice exposed to peritoneal injection of LPS (2X LPS) are similar between the two genotypes.

Previous studies suggested that increased microglial expression of the myeloid lineage-determining factor PU.1 (encoded by the *Spi-1* gene)—a master regulator of microglia development and function—might underly an exacerbated response to pro-inflammatory stimulation in HD microglia from knock-in (Q175) and fragment (R6/2) HD models [12]. In line with our finding of a normal response of Q140/140 microglia to pro-inflammatory stimulation in vitro and in vivo, we also found that *Spi-1* expression was similar in Q140/140 and Q7/7 microglia. These data also confirm our previous observation of normal *Spi-1* expression in the brain of R6/2 mice [36]. We speculate that previously reported increases in the expression of *Spi-1* in HD microglia might have resulted from non-cell autonomous microglia exposure to environmental triggers, including pathogens and/or gut microbiota that could indirectly cause microglia priming in vivo [87]. This appears to be even more likely considering the emerging evidence of a gut-immune system-brain axis with the potential to modulate neuroinflammation and behaviour in HD and other neurodegenerative disorders [88–90].

In our experiments, we noticed that incubation with necrotic cells carrying mutant HTT (97Q) induced a higher expression of *Il-1b* and *Il-6* compared to necrotic cells expressing wild-type HTT (25Q). This suggests that along with classic DAMPs and other mediators of inflammation, HD cells might release additional factors that increase microglia activation, including mutant HTT itself. In support of a higher inflammogenic potential of necrotic HD cells, N2a cells carrying mutant HTT were previously shown to produce higher levels of inflammatory molecules such as MCP-1 and IL-6 compared to wild-type N2a cells [33].

Innate immune tolerance is developed as part of the brain response to acute injuries such as ischemia [91–93] and might limit brain damage and chronic inflammation in neuroinflammatory and neurodegenerative conditions [51, 68, 94]. In our experiments, Q7/7 microglia were able to acquire a tolerant state characterized by a lower expression of pro-inflammatory cytokine upon a second exposure to LPS. In contrast, in Q140/140 microglia, only TNF was silenced, but not IL-1β and IL-6, the expression of which remained as high as after the first stimulation with LPS. The fact that the transcription of *Il-1b* and *Il-6* was affected differently from *Tnf* is not surprising, since chromatin remodelling and epigenetic marks that lead to gene silencing in tolerant cells are gene- and context-specific [69], and the *Il-1b* gene might be less sensitive to the establishment of endotoxin tolerance compared to the *Tnf* gene [95]. In vivo studies confirmed that the development of innate immune tolerance in the brain is impaired, or at least delayed in Q140/140 mice, the latter being less responsive to tolerizing stimuli compared to Q7/7 mice, reducing the production of several pro-inflammatory cytokines (with the exception of GM-CSF and INF-γ) by brain cells to a lesser extent than Q7/7, and requiring additional exposure to tolerizing conditions to achieve the same degree of tolerance as Q7/7 mice. Although the complexity of the brain milieu might affect microglia responses in vivo, and other brain cells might contribute to the overall levels of cytokines measured in the brain in vivo [33, 96–101], the fact that tolerance is also impaired in isolated microglia in vitro clearly suggests that this aberrant phenotype develops in Q140/140 microglia in a cell-autonomous manner.

TLR4 expression at the plasma membrane, which could potentially affect the strength of the tolerogenic signaling, was normal in Q140/140 microglia, as assessed in our in vitro studies. Furthermore, priming of the *Fpr1* gene, another consequence of multiple LPS stimulations [69], was not affected in Q140/140 cells, confirming that TLR4 activation occurred as expected. Other potential players in the development of tolerance, such as the tolerogenic cytokines IL-10 and TGFβ [70, 102, 103] were not likely to be involved either, since their expression in Q140/140 microglia was similar or even higher (for IL-10) compared to Q7/7 microglia. IL-10 levels were also similar in the brain of Q140/140 and Q7/7 mice. Therefore, the reason of impaired or delayed tolerance in Q140/140 microglia remains to be determined. Perhaps, altered epigenetic mechanisms induced by mutant HTT might interfere with the specific epigenetic modifications, including histone deacetylation and H3K4 demethylation, that drive gene silencing and the development

of tolerance [69]. Expression of mHTT is indeed associated with epigenetic modifications in hundreds of genes, although most of these tend to repress gene expression [104, 105] and, therefore, would not explain why Q140/140 microglia failed to silence *Il-6* and *Il-1b* in our in vitro experiments, and to decrease the expression of many other pro-inflammatory molecules to the same extent as Q7/7 after 3 LPS stimulations.

Altogether, our data suggest that an impairment (or a delay) in the ability of HD microglia to develop tolerance, rather than cell-autonomous spontaneous activation or stimulus-induced overactivation of naïve HD microglia, might contribute to a chronic inflammatory state in HD. Impaired or delayed tolerance might also explain some of the inconsistencies across different studies in the detection of HD microglia activation, as it could confound data interpretation in animal models exposed to pathogens or dysbiosis. On the other hand, in a pathogen-free environment, the inflammatory potential of microglia that express wild-type or mutant HTT might be similar, at least at early disease stages and in the absence of activating DAMPs, a hypothesis that is also supported by studies that showed that selective depletion of mutant HTT in microglia of BACHD mice, likely maintained in a controlled and clean, pathogen-free environment, did not affect mouse phenotype and pathology [106].

Recently, O'Regan et al. [107] evaluated the inflammatory phenotype of microglia-like cells differentiated from isogenic human iPSCs expressing HTT with polyQ expansions of various lengths. They reported that microglia-like cells with a polyQ expansion (81Q) that is usually linked to juvenile HD, expressed higher levels of IL-6 and TNF following LPS stimulation (1 μg/ml) compared to cells bearing HTT with a normal polyQ length (30Q). However, in cells expressing mutant HTT with 45Q (resulting in adult-onset HD), the secretion of these cytokines was not significantly different from control cells (30Q) [107]. Therefore, it is possible that HD microglia might have a higher inflammogenic potential in the context of juvenile HD, but not in adult-onset HD. Further studies with a much larger number of iPSC lines would be required to test this hypothesis. Q140 mice and similar models that express full-length mHTT more closely mirror adult-onset HD, in spite of the larger CAG expansions they carry in their *Htt* gene.

Even if not caused by cell-autonomous effects of mutant HTT expression, microglia activation and the establishment of neuroinflammation with disease progression [28] are likely to contribute to pathology in HD [108] and are a potential target for intervention. In support of this hypothesis, a few studies showed that decreasing glia activation and production of pro-inflammatory cytokines has beneficial effects in HD mouse models: the knock-out of TLR2 or TLR4 extended the life-span of N171-82Q mice [45], a model that overexpresses an N-terminal fragment of mutant HTT in neurons only [109], while inhibition of IKK and the NFkB pathway [110] or TNF signaling [79] in R6/2 mice decreased neurodegeneration and improved mouse behaviour.

We previously showed that the production of pro-inflammatory cytokines by normal murine and human microglia is modulated by endogenous gangliosides and can be drastically decreased by administration of ganglioside GM1 [53]. Gangliosides are glycosphingolipids present at the plasma membrane of all cells and are particularly abundant in the brain [111]. They play many roles as modulators of cell signaling and immune functions [112, 113], and have profound neuroprotective and disease-modifying effects in HD models [36, 114, 115], where levels of GM1 and other gangliosides were found to be decreased [115, 116]. Whether GM1 would exert on HD microglia the same anti-inflammatory effects that it exerts on wild-type microglia was not known, and yet crucial to determine, as expression of mutant HTT could potentially alter pathways and mediators involved in the anti-inflammatory action of gangliosides. Treatment of HD microglia with GM1 significantly decreased the expression of pro-inflammatory cytokines and the production of reactive nitrite following microglia stimulation with LPS and LTA. Of note, GM1 decreased the expression of all major pro-inflammatory cytokines upon microglia exposure to repeated LPS stimulations in our experimental model of tolerance. Interestingly, GM1 treatment also resulted in the down-regulation of a prototypical non-tolerizeable gene, *Fpr1*, in both Q7/Q7 and Q140/140 microglia. This suggests that rather than restoring gene silencing of tolerizeable genes in Q140/140 microglia, cell pre-incubation with the ganglioside might block stimulation by LPS altogether, as also shown in our previous studies in wild-type microglia [53].

The exact mechanisms underlying the anti-inflammatory effects of GM1 in normal and HD microglia awaits clarification. Our previous studies showed that GM1 administration decreases the activation of both NFkB and MAPK pathways required for pro-inflammatory cytokine expression and secretion [117–120], without significantly altering TLR4 levels [53]. Furthermore, GM1 exerts its effects even after microglia incubation with LPS, suggesting that it must attenuate signaling downstream of TLR4 activation. We showed that both the ceramide tail of gangliosides and the specific composition of the glycan head group, including the presence of sialic acid, are required to mediate anti-inflammatory effects [53], suggesting that glycan-binding proteins, in particular sialic-acid binding proteins, might interact with gangliosides in a glycan-specific

manner to mediate their signaling effects. Another potential mechanism could be through NFkB sequestration in lipid rafts, which represses NFkB signaling [121]. The effects of GM1 pre-incubation (24 h recovery period) in our experimental model of tolerance are particularly profound and might not necessarily occur with the same mechanism that dampens the expression of inflammatory molecules when GM1 is administered for a shorter time after cell stimulation with LPS. Gangliosides were shown to upregulate the expression of IRAK-3 in monocytes [74]. IRAK-3 is a negative regulator of TLR4 signaling [122] and it is involved in endotoxin tolerance [75, 76, 123] and the epigenetic suppression of tolerizeable genes [124]. In our studies, *Irak-3* expression was similar between Q140/140 and Q7/7 microglia in all conditions tested (naïve or tolerized), and it was not affected by treatment of naïve microglia with GM1. In our tolerance model, GM1 dramatically decreased, rather than increasing, *Irak-3* expression. Because *Irak-3* is itself a target of TLR-signaling [122], the failure of cells treated with GM1 to upregulate this gene might be in line with the powerful inhibitory effects of GM1 on microglia re-stimulation with LPS in our tolerance experiments. Therefore, an IRAK-3-independent mechanism underlies the effects of GM1 on microglia activation, reactivation and tolerance. Further investigations are warranted to shed light on such mechanism.

In summary, our studies suggests that expression of mutant HTT in HD microglia does not result, per se, in a heightened microglia response to inflammatory stimuli, at least in a model of adult-onset HD, but causes a cell-autonomous impairment in the development of tolerance that might enable chronic inflammation in the brain and, in turn, contribute to disease progression. GM1 administration exerts potent anti-inflammatory effects that might be beneficial in HD patients to decrease neuroinflammation.

Abbreviations

FDR	Formyl peptide receptor 1
GM-CSF	Granulocite-macrophagy colony-stimulating factor
HD	Huntington's disease
IL-1β	Interleukin-1β
IL-1α	Interleukin-1α
IL-6	Interleukin-6
IRAK-3	Interleukin 1 receptor associated kinase 3
KC	Keratinocyte-derived chemokine
LDH	Lactic dehydrogenase
LIX	LPS-induced CXC chemokine
LPS	Lipopolysaccharide
MAPK	Mitogen-activated protein kinase
MCP1	Monocyte chemoattractant protein-1
NFκB	Nuclear factor NF-kappa-B
NO	Nitric oxide
TNF	Tumor necrosis factor
TLR4	Toll-like receptor 4
TLR2	Toll-like receptor 2

Supplementary Information

The online version contains supplementary material available at https://doi.org/10.1186/s12974-023-02963-y.

Additional file 1: Fig. S1. Q7/7 and Q140/140 microglia express similar levels of TLR4 and TLR2 at the plasma membrane in naïve and stimulated conditions. (A) Schematic representation and timeline of cell treatment with LPS. Representative histograms and relative flow cytometry quantification (% $TLR4^+$-cells and median fluorescence intensity) of plasma membrane TLR4 in naïve microglia (I), after 12 h of exposure to LPS (100 ng/ml) (II), and after LPS removal and 24 h of recovery in serum-free medium (III). N ≥ 5. A two-sided unpaired *t*-test was used to compare TLR4 levels between genotypes. (B) Plasma membrane TLR2 was measured by flow cytometry in naïve microglia (I) and after 6 h of LTA (10 ug/ml) stimulation (II). Representative histograms and quantification of $TLR2^+$-cells and TLR2 median fluorescence intensity are shown in the bar graphs. N ≥ 3. Two-way ANOVA with Tukey's multiple comparisons test. Bars are means ± STDEV. **Fig. S2.** LPS treatment does not significantly affect the survival of Q7/7 and Q140/140 microglia. Representative images of Q140/140 microglia stained with Hoechst (blue) and PI (yellow) after incubation in serum-free medium for 24 h (top panels), and Metaxpress software masks (bottom panels) used for the automated quantification of cell nuclei and propidium iodide (PI)-positive cells (dead cells) by high-content microscopy analysis of cell death. Scale bar = 150 µm. The graph shows the % of PI-positive cells in microglia cultures treated with or without LPS (100 ng/ml) for 24 and 48 h. N = 4. Two-way ANOVA with Tukey's post test. **Fig. S3.** Necrotic N2a cells carrying mutant HTT induce higher microglial expression of pro-inflammatory cytokines compared to necrotic cells carrying wild-type HTT. Q7/7 and Q140/140 microglia were incubated with necrotic N2a25Q (25Q, wild-type HTT) or N2a97Q (97Q, mutant HTT) cells for 4 h (1:2 microglia to necrotic cells ratio). Graphs show the fold-change of pro-inflammatory cytokine gene expression compared to the expression induced by necrotic N2a25Q cells. mRNA levels of the indicated cytokines were normalized over the geometric mean of three housekeeping genes (Normalization Index) (N ≥ 4). Ratio paired *t*-test. $*p < 0.05$. **Fig. S4.** Comparable levels of cell death in Q7/7 and Q140/140 microglia after exposure to LPS and recovery. LDH enzymatic activity released in the culture medium due to cell death was measured in microglia cultures incubated with or without LPS (100 ng/ml) for 12 h (A) and after 24 h recovery in serum-free medium. N = 3. (B) Two-way ANOVA with Tukey's multiple comparisons test. Bars are means ± STDEV. $*p < 0.05$. **Fig. S5 .** GM1 decreases expression and production of pro-inflammatory cytokines in Q7/7 microglia. Q7/7 microglia were activated with LPS (100 ng/ml) for 3 h, washed and treated with GM1 (50 µM) for 6 h. GM1 reduced the levels of (A) *Il-1b* and *Tnf* mRNA (N = 5), and (B) TNF secreted in the medium (N ≥ 3). Gene expression was normalized over *Ppia*. Two-way ANOVA with Tukey's multiple comparisons test was used. $*p < 0.05$; $**p < 0.01$; $***p < 0.001$, $****p < 0.0001$. **Fig. S6.** GM1 does not affect *Irak-3* expression in naïve Q7/7 and Q14/140 microglia. Naïve microglia were incubated with GM1 in serum-free medium for 8 h prior to RNA extraction and analysis of Irak-3 mRNA levels. Irak-3 expression was normalized over the geometric mean of three housekeeping genes. No statistically significant differences were detected among groups. N ≥ 3. Bars are means ± STDEV. Two-way ANOVA with Tukey's multiple comparisons test.

Acknowledgements

We thank TRB Chemedica Inc. for the gift of GM1. Schematics were generated using BioRender.com.

Author contributions

NS, SS and DG designed research and experiments; NS, DG, and AZ performed experiments and analyzed data; MH performed experiments; SS supervised experiments and data analysis. NS and SS wrote the manuscript; all authors read and approved the final manuscript.

Funding
This work was supported by grants from Brain Canada/Huntington Society of Canada, the Natural Sciences and Engineering Research Council of Canada (NSERC), the Canadian Institutes of Health Research (CIHR) and Synergies in Alzheimer's Disease. Experiments were performed at the University of Alberta Faculty of Medicine and Dentistry Flow Cytometry Core and Oncology Microscopy Core, which receive financial support from the Faculty of Medicine and Dentistry and Canada Foundation for Innovation (CF) awards to contributing investigators. NS was supported by a Faculty of Medicine and Dentistry Dean's Studentship, an Alzheimer's Disease and Related Dementias studentship and the Alberta Graduate Excellence Scholarship.

Availability of data and materials
All data generated or analysed during this study are included in this published article and its supplementary information files.

Declarations

Ethics approval and consent to participate
All procedures on animals were approved by the University of Alberta Animal Care and Use Committee (AUP00000336) and were in accordance with the guidelines of the Canadian Council on Animal Care.

Consent for publication
Not applicable.

Competing interests
SS and the University of Alberta hold a patent for the use of GM1 in HD. There are no other competing interests to declare.

Author details
[1]Department of Pharmacology, Neuroscience and Mental Health Institute and Glycomics Institute of Alberta, University of Alberta, Edmonton, AB, Canada. [2]Present Address: Department of Neurology, Johns Hopkins University School of Medicine, Baltimore, MD, USA.

Received: 7 March 2023 Accepted: 18 November 2023
Published online: 23 November 2023

References

1. Reiner A, Dragatsis I, Dietrich P. Genetics and neuropathology of Huntington's disease. Int Rev Neurobiol. 2011;98:325–72.
2. A novel gene containing a trinucleotide repeat that is expanded and unstable on Huntington's disease chromosomes. The Huntington's Disease Collaborative Research Group. Cell. 1993;72(6):971–83.
3. Warby SC, Montpetit A, Hayden AR, Carroll JB, Butland SL, Visscher H, et al. CAG expansion in the Huntington disease gene is associated with a specific and targetable predisposing haplogroup. Am J Hum Genet. 2009;84(3):351–66.
4. Tabrizi SJ, Flower MD, Ross CA, Wild EJ. Huntington disease: new insights into molecular pathogenesis and therapeutic opportunities. Nat Rev Neurol. 2020;16(10):529–46.
5. Hazeki N, Nakamura K, Goto J, Kanazawa I. Rapid aggregate formation of the huntingtin N-terminal fragment carrying an expanded polyglutamine tract. Biochem Biophys Res Commun. 1999;256(2):361–6.
6. Wang CE, Tydlacka S, Orr AL, Yang SH, Graham RK, Hayden MR, et al. Accumulation of N-terminal mutant huntingtin in mouse and monkey models implicated as a pathogenic mechanism in Huntington's disease. Hum Mol Genet. 2008;17(17):2738–51.
7. Juenemann K, Schipper-Krom S, Wiemhoefer A, Kloss A, Sanz Sanz A, Reits EAJ. Expanded polyglutamine-containing N-terminal huntingtin fragments are entirely degraded by mammalian proteasomes. J Biol Chem. 2013;288(38):27068–84.
8. Strong TV, Tagle DA, Valdes JM, Elmer LW, Boehm K, Swaroop M, et al. Widespread expression of the human and rat Huntington's disease gene in brain and nonneural tissues. Nat Genet. 1993;5(3):259–65.
9. Li SH, Schilling G, Young WS 3rd, Li XJ, Margolis RL, Stine OC, et al. Huntington's disease gene (IT15) is widely expressed in human and rat tissues. Neuron. 1993;11(5):985–93.
10. Landwehrmeyer GB, McNeil SM, Dure LST, Ge P, Aizawa H, Huang Q, et al. Huntington's disease gene: regional and cellular expression in brain of normal and affected individuals. Ann Neurol. 1995;37(2):218–30.
11. Shin JY, Fang ZH, Yu ZX, Wang CE, Li SH, Li XJ. Expression of mutant huntingtin in glial cells contributes to neuronal excitotoxicity. J Cell Biol. 2005;171(6):1001–12.
12. Crotti A, Benner C, Kerman BE, Gosselin D, Lagier-Tourenne C, Zuccato C, et al. Mutant Huntingtin promotes autonomous microglia activation via myeloid lineage-determining factors. Nat Neurosci. 2014;17(4):513–21.
13. Ferrari Bardile C, Garcia-Miralles M, Caron NS, Rayan NA, Langley SR, Harmston N, et al. Intrinsic mutant HTT-mediated defects in oligodendroglia cause myelination deficits and behavioral abnormalities in Huntington disease. Proc Natl Acad Sci U S A. 2019;116(19):9622–7.
14. Faideau M, Kim J, Cormier K, Gilmore R, Welch M, Auregan G, et al. In vivo expression of polyglutamine-expanded huntingtin by mouse striatal astrocytes impairs glutamate transport: a correlation with Huntington's disease subjects. Hum Mol Genet. 2010;19(15):3053–67.
15. Li Q, Barres BA. Microglia and macrophages in brain homeostasis and disease. Nat Rev Immunol. 2018;18(4):225–42.
16. Sierra A, Paolicelli RC, Kettenmann H. Cien anos de microglia: milestones in a century of microglial research. Trends Neurosci. 2019;42(11):778–92.
17. Thion MS, Garel S. Microglial ontogeny, diversity and neurodevelopmental functions. Curr Opin Genet Dev. 2020;65:186–94.
18. Davis EJ, Foster TD, Thomas WE. Cellular forms and functions of brain microglia. Brain Res Bull. 1994;34(1):73–8.
19. Tian L, Ma L, Kaarela T, Li Z. Neuroimmune crosstalk in the central nervous system and its significance for neurological diseases. J Neuroinflamm. 2012;9:155.
20. Streit WJ. Microglial response to brain injury: a brief synopsis. Toxicol Pathol. 2000;28(1):28–30.
21. Lively S, Schlichter LC. Microglia responses to pro-inflammatory stimuli (LPS, IFNgamma+TNFalpha) and reprogramming by resolving cytokines (IL-4, IL-10). Front Cell Neurosci. 2018;12:215.
22. Lucin KM, Wyss-Coray T. Immune activation in brain aging and neurodegeneration: too much or too little? Neuron. 2009;64(1):110–22.
23. Heneka MT, Kummer MP, Latz E. Innate immune activation in neurodegenerative disease. Nat Rev Immunol. 2014;14(7):463–77.
24. Ransohoff RM. How neuroinflammation contributes to neurodegeneration. Science. 2016;353(6301):777–83.
25. Politis M, Lahiri N, Niccolini F, Su P, Wu K, Giannetti P, et al. Increased central microglial activation associated with peripheral cytokine levels in premanifest Huntington's disease gene carriers. Neurobiol Dis. 2015;83:115–21.
26. Tai YF, Pavese N, Gerhard A, Tabrizi SJ, Barker RA, Brooks DJ, Piccini P. Imaging microglial activation in Huntington's disease. Brain Res Bull. 2007;72(2–3):148–51.
27. Tai YF, Pavese N, Gerhard A, Tabrizi SJ, Barker RA, Brooks DJ, Piccini P. Microglial activation in presymptomatic Huntington's disease gene carriers. Brain. 2007;130(Pt 7):1759–66.
28. Pavese N, Gerhard A, Tai YF, Ho AK, Turkheimer F, Barker RA, et al. Microglial activation correlates with severity in Huntington disease: a clinical and PET study. Neurology. 2006;66(11):1638–43.
29. Bragg RM, Coffey SR, Weston RM, Ament SA, Cantle JP, Minnig S, et al. Motivational, proteostatic and transcriptional deficits precede synapse loss, gliosis and neurodegeneration in the B6.Htt(Q111/+) model of Huntington's disease. Sci Rep. 2017;7:41570.
30. Coffey SR, Bragg RM, Minnig S, Ament SA, Cantle JP, Glickenhaus A, et al. Peripheral huntingtin silencing does not ameliorate central signs of disease in the B6HttQ111/+ mouse model of Huntington's disease. PLoS ONE. 2017;12(4): e0175968.
31. Johnson E, Chase K, McGowan S, Mondo E, Pfister E, Mick E, et al. Safety of striatal infusion of siRNA in a transgenic Huntington's disease mouse model. J Huntington's Dis. 2015;4(3):219–29.
32. Franciosi S, Ryu JK, Shim Y, Hill A, Connolly C, Hayden MR, et al. Age-dependent neurovascular abnormalities and altered microglial

morphology in the YAC128 mouse model of Huntington disease. Neurobiol Dis. 2012;45(1):438–49.
33. Godavarthi SK, Narender D, Mishra A, Goswami A, Rao SN, Nukina N, Jana NR. Induction of chemokines, MCP-1, and KC in the mutant huntingtin expressing neuronal cells because of proteasomal dysfunction. J Neurochem. 2009;108(3):787–95.
34. Ma L, Morton AJ, Nicholson LF. Microglia density decreases with age in a mouse model of Huntington's disease. Glia. 2003;43(3):274–80.
35. Zwilling D, Huang SY, Sathyasaikumar KV, Notarangelo FM, Guidetti P, Wu HQ, et al. Kynurenine 3-monooxygenase inhibition in blood ameliorates neurodegeneration. Cell. 2011;145(6):863–74.
36. Alpaugh M, Galleguillos D, Forero J, Morales LC, Lackey SW, Kar P, et al. Disease-modifying effects of ganglioside GM1 in Huntington's disease models. EMBO Mol Med. 2017;9(11):1537–57.
37. Paldino E, Balducci C, La Vitola P, Artioli L, D'Angelo V, Giampa C, et al. Neuroprotective effects of doxycycline in the R6/2 mouse model of Huntington's disease. Mol Neurobiol. 2020;57(4):1889–903.
38. Joshi AU, Minhas PS, Liddelow SA, Haileselassie B, Andreasson KI, Dorn GW 2nd, Mochly-Rosen D. Fragmented mitochondria released from microglia trigger A1 astrocytic response and propagate inflammatory neurodegeneration. Nat Neurosci. 2019;22(10):1635–48.
39. Savage JC, St-Pierre MK, Carrier M, El Hajj H, Novak SW, Sanchez MG, et al. Microglial physiological properties and interactions with synapses are altered at presymptomatic stages in a mouse model of Huntington's disease pathology. J Neuroinflamm. 2020;17(1):98.
40. Crapser JD, Ochaba J, Soni N, Reidling JC, Thompson LM, Green KN. Microglial depletion prevents extracellular matrix changes and striatal volume reduction in a model of Huntington's disease. Brain. 2020;143(1):266–88.
41. Simmons DA, Casale M, Alcon B, Pham N, Narayan N, Lynch G. Ferritin accumulation in dystrophic microglia is an early event in the development of Huntington's disease. Glia. 2007;55(10):1074–84.
42. Simmons DA, James ML, Belichenko NP, Semaan S, Condon C, Kuan J, et al. TSPO-PET imaging using [18F]PBR06 is a potential translatable biomarker for treatment response in Huntington's disease: preclinical evidence with the p75NTR ligand LM11A-31. Hum Mol Genet. 2018;27(16):2893–912.
43. Bjorkqvist M, Wild EJ, Thiele J, Silvestroni A, Andre R, Lahiri N, et al. A novel pathogenic pathway of immune activation detectable before clinical onset in Huntington's disease. J Exp Med. 2008;205(8):1869–77.
44. Ferrante RJ. Mouse models of Huntington's disease and methodological considerations for therapeutic trials. Biochim Biophys Acta. 2009;1792(6):506–20.
45. Griffioen K, Mattson MP, Okun E. Deficiency of Toll-like receptors 2, 3 or 4 extends life expectancy in Huntington's disease mice. Heliyon. 2018;4(1): e00508.
46. Fiebich BL, Batista CRA, Saliba SW, Yousif NM, de Oliveira ACP. Role of microglia TLRs in neurodegeneration. Front Cell Neurosci. 2018;12:329.
47. Gorman AM. Neuronal cell death in neurodegenerative diseases: recurring themes around protein handling. J Cell Mol Med. 2008;12(6A):2263–80.
48. Chi H, Chang HY, Sang TK. Neuronal cell death mechanisms in major neurodegenerative diseases. Int J Mol Sci. 2018. https://doi.org/10.3390/ijms19103082.
49. Lehner MD, Morath S, Michelsen KS, Schumann RR, Hartung T. Induction of cross-tolerance by lipopolysaccharide and highly purified lipoteichoic acid via different toll-like receptors independent of paracrine mediators. J Immunol. 2001;166(8):5161–7.
50. Schaafsma W, Zhang X, van Zomeren KC, Jacobs S, Georgieva PB, Wolf SA, et al. Long-lasting pro-inflammatory suppression of microglia by LPS-preconditioning is mediated by RelB-dependent epigenetic silencing. Brain Behav Immun. 2015;48:205–21.
51. Wendeln AC, Degenhardt K, Kaurani L, Gertig M, Ulas T, Jain G, et al. Innate immune memory in the brain shapes neurological disease hallmarks. Nature. 2018;556(7701):332–8.
52. Cherry JD, Olschowka JA, O'Banion MK. Neuroinflammation and M2 microglia: the good, the bad, and the inflamed. J Neuroinflamm. 2014;11:98.
53. Galleguillos D, Wang Q, Steinberg N, Zaidi A, Shrivastava G, Dhami K, et al. Anti-inflammatory role of GM1 and other gangliosides on microglia. J Neuroinflamm. 2022;19(1):9.
54. Menalled LB, Sison JD, Dragatsis I, Zeitlin S, Chesselet MF. Time course of early motor and neuropathological anomalies in a knock-in mouse model of Huntington's disease with 140 CAG repeats. J Comp Neurol. 2003;465(1):11–26.
55. Saura J, Tusell JM, Serratosa J. High-yield isolation of murine microglia by mild trypsinization. Glia. 2003;44(3):183–9.
56. Durafourt BA, Moore CS, Zammit DA, Johnson TA, Zaguia F, Guiot MC, et al. Comparison of polarization properties of human adult microglia and blood-derived macrophages. Glia. 2012;60(5):717–27.
57. Pal R, Bradford BM, Mabbott NA. Innate immune tolerance in microglia does not impact on central nervous system prion disease. Front Cell Neurosci. 2022;16: 918883.
58. Puntener U, Booth SG, Perry VH, Teeling JL. Long-term impact of systemic bacterial infection on the cerebral vasculature and microglia. J Neuroinflamm. 2012;9:146.
59. Jesudasan SJB, Gupta SJ, Churchward MA, Todd KG, Winship IR. Inflammatory cytokine profile and plasticity of brain and spinal microglia in response to ATP and glutamate. Front Cell Neurosci. 2021;15: 634020.
60. Vandesompele J, De Preter K, Pattyn F, Poppe B, Van Roy N, De Paepe A, Speleman F. Accurate normalization of real-time quantitative RT-PCR data by geometric averaging of multiple internal control genes. Genome Biol. 2002;3(7):RESEARCH0034.
61. Li M, Carpio DF, Zheng Y, Bruzzo P, Singh V, Ouaaz F, et al. An essential role of the NF-kappa B/Toll-like receptor pathway in induction of inflammatory and tissue-repair gene expression by necrotic cells. J Immunol. 2001;166(12):7128–35.
62. Ho J, Tumkaya T, Aryal S, Choi H, Claridge-Chang A. Moving beyond P values: data analysis with estimation graphics. Nat Methods. 2019;16(7):565–6.
63. Long EM, Millen B, Kubes P, Robbins SM. Lipoteichoic acid induces unique inflammatory responses when compared to other toll-like receptor 2 ligands. PLoS ONE. 2009;4(5): e5601.
64. Jana M, Palencia CA, Pahan K. Fibrillar amyloid-beta peptides activate microglia via TLR2: implications for Alzheimer's disease. J Immunol. 2008;181(10):7254–62.
65. Scheiblich H, Bousset L, Schwartz S, Griep A, Latz E, Melki R, Heneka MT. Microglial NLRP3 inflammasome activation upon TLR2 and TLR5 ligation by distinct alpha-synuclein assemblies. J Immunol. 2021;207(8):2143–54.
66. Kim C, Ho DH, Suk JE, You S, Michael S, Kang J, et al. Neuron-released oligomeric alpha-synuclein is an endogenous agonist of TLR2 for paracrine activation of microglia. Nat Commun. 2013;4:1562.
67. Liu S, Liu Y, Hao W, Wolf L, Kiliaan AJ, Penke B, et al. TLR2 is a primary receptor for Alzheimer's amyloid beta peptide to trigger neuroinflammatory activation. J Immunol. 2012;188(3):1098–107.
68. Kucuksezer UC, Ozdemir C, Akdis M, Akdis CA. Influence of innate immunity on immune tolerance. Acta Med Acad. 2020;49(2):164–80.
69. Foster SL, Hargreaves DC, Medzhitov R. Gene-specific control of inflammation by TLR-induced chromatin modifications. Nature. 2007;447(7147):972–8.
70. Lajqi T, Lang GP, Haas F, Williams DL, Hudalla H, Bauer M, et al. Memory-like inflammatory responses of microglia to rising doses of LPS: key role of PI3Kgamma. Front Immunol. 2019;10:2492.
71. Laffer B, Bauer D, Wasmuth S, Busch M, Jalilvand TV, Thanos S, et al. Loss of IL-10 promotes differentiation of microglia to a M1 phenotype. Front Cell Neurosci. 2019;13:430.
72. Frei K, Lins H, Schwerdel C, Fontana A. Antigen presentation in the central nervous system. The inhibitory effect of IL-10 on MHC class II expression and production of cytokines depends on the inducing signals and the type of cell analyzed. J Immunol. 1994;152(6):2720–8.
73. Ledeboer A, Breve JJ, Poole S, Tilders FJ, Van Dam AM. Interleukin-10, interleukin-4, and transforming growth factor-beta differentially regulate lipopolysaccharide-induced production of pro-inflammatory cytokines and nitric oxide in co-cultures of rat astroglial and microglial cells. Glia. 2000;30(2):134–42.
74. Shen W, Stone K, Jales A, Leitenberg D, Ladisch S. Inhibition of TLR activation and up-regulation of IL-1R-associated kinase-M expression by exogenous gangliosides. J Immunol. 2008;180(7):4425–32.
75. Nakayama K, Okugawa S, Yanagimoto S, Kitazawa T, Tsukada K, Kawada M, et al. Involvement of IRAK-M in peptidoglycan-induced tolerance in macrophages. J Biol Chem. 2004;279(8):6629–34.

76. van Veer C, van den Pangaart PS, van Zoelen MA, de Kruif M, Birjmohun RS, Stroes ES, et al. Induction of IRAK-M is associated with lipopolysaccharide tolerance in a human endotoxemia model. J Immunol. 2007;179(10):7110–20.
77. Liu ZJ, Yan LN, Li XH, Xu FL, Chen XF, You HB, Gong JP. Up-regulation of IRAK-M is essential for endotoxin tolerance induced by a low dose of lipopolysaccharide in Kupffer cells. J Surg Res. 2008;150(1):34–9.
78. Siew JJ, Chen HM, Chen HY, Chen HL, Chen CM, Soong BW, et al. Galectin-3 is required for the microglia-mediated brain inflammation in a model of Huntington's disease. Nat Commun. 2019;10(1):3473.
79. Hsiao HY, Chiu FL, Chen CM, Wu YR, Chen HM, Chen YC, et al. Inhibition of soluble tumor necrosis factor is therapeutic in Huntington's disease. Hum Mol Genet. 2014;23(16):4328–44.
80. Lehnardt S, Massillon L, Follett P, Jensen FE, Ratan R, Rosenberg PA, et al. Activation of innate immunity in the CNS triggers neurodegeneration through a Toll-like receptor 4-dependent pathway. Proc Natl Acad Sci U S A. 2003;100(14):8514–9.
81. Cui W, Sun C, Ma Y, Wang S, Wang X, Zhang Y. Inhibition of TLR4 induces M2 microglial polarization and provides neuroprotection via the NLRP3 inflammasome in Alzheimer's disease. Front Neurosci. 2020;14:444.
82. Chen K, Iribarren P, Hu J, Chen J, Gong W, Cho EH, et al. Activation of Toll-like receptor 2 on microglia promotes cell uptake of Alzheimer disease-associated amyloid beta peptide. J Biol Chem. 2006;281(6):3651–9.
83. Pascual M, Calvo-Rodriguez M, Núñez L, Villalobos C, Ureña J, Guerri C. Toll-like receptors in neuroinflammation, neurodegeneration, and alcohol-induced brain damage. IUBMB Life. 2021;73(7):900–15.
84. Venegas C, Heneka MT. Danger-associated molecular patterns in Alzheimer's disease. J Leukoc Biol. 2017;101(1):87–98.
85. Marsh BJ, Williams-Karnesky RL, Stenzel-Poore MP. Toll-like receptor signaling in endogenous neuroprotection and stroke. Neuroscience. 2009;158(3):1007–20.
86. Pais TF, Figueiredo C, Peixoto R, Braz MH, Chatterjee S. Necrotic neurons enhance microglial neurotoxicity through induction of glutaminase by a MyD88-dependent pathway. J Neuroinflamm. 2008;5:43.
87. Perry VH, Holmes C. Microglial priming in neurodegenerative disease. Nat Rev Neurol. 2014;10(4):217–24.
88. Love CJ, Masson BA, Gubert C, Hannan AJ. The microbiota-gut-brain axis in Huntington's disease. Int Rev Neurobiol. 2022;167:141–84.
89. Singh A, Dawson TM, Kulkarni S. Neurodegenerative disorders and gut–brain interactions. J Clin Invest. 2021. https://doi.org/10.1172/JCI143775.
90. Chongtham A, Yoo JH, Chin TM, Akingbesote ND, Huda A, Marsh JL, Khoshnan A. Gut bacteria regulate the pathogenesis of Huntington's disease in drosophila model. Front Neurosci. 2022;16: 902205.
91. Rosenzweig HL, Lessov NS, Henshall DC, Minami M, Simon RP, Stenzel-Poore MP. Endotoxin preconditioning prevents cellular inflammatory response during ischemic neuroprotection in mice. Stroke J Cereb Circ. 2004;35(11):2576–81.
92. Wang YC, Lin S, Yang QW. Toll-like receptors in cerebral ischemic inflammatory injury. J Neuroinflamm. 2011;8:134.
93. Kariko K, Weissman D, Welsh FA. Inhibition of toll-like receptor and cytokine signaling—a unifying theme in ischemic tolerance. J Cereb Blood Flow Metab. 2004;24(11):1288–304.
94. Neher JJ, Cunningham C. Priming microglia for innate immune memory in the brain. Trends Immunol. 2019;40(4):358–74.
95. Adamik J, Wang KZ, Unlu S, Su AJ, Tannahill GM, Galson DL, et al. Distinct mechanisms for induction and tolerance regulate the immediate early genes encoding interleukin 1beta and tumor necrosis factor alpha. PLoS ONE. 2013;8(8): e70622.
96. Cekanaviciute E, Buckwalter MS. Astrocytes: integrative regulators of neuroinflammation in stroke and other neurological diseases. Neurotherapeutics. 2016;13(4):685–701.
97. Choi SS, Lee HJ, Lim I, Satoh J, Kim SU. Human astrocytes: secretome profiles of cytokines and chemokines. PLoS ONE. 2014;9(4): e92325.
98. Hyvarinen T, Hagman S, Ristola M, Sukki L, Veijula K, Kreutzer J, et al. Co-stimulation with IL-1beta and TNF-alpha induces an inflammatory reactive astrocyte phenotype with neurosupportive characteristics in a human pluripotent stem cell model system. Sci Rep. 2019;9(1):16944.
99. Pugazhenthi S, Zhang Y, Bouchard R, Mahaffey G. Induction of an inflammatory loop by interleukin-1beta and tumor necrosis factor-alpha involves NF-kB and STAT-1 in differentiated human neuroprogenitor cells. PLoS ONE. 2013;8(7): e69585.
100. Yang J, Li Y, Bhalla A, Maienschein-Cline M, Fukuchi KI. A novel co-culture model for investigation of the effects of LPS-induced macrophage-derived cytokines on brain endothelial cells. PLoS ONE. 2023;18(7): e0288497.
101. O'Carroll SJ, Kho DT, Wiltshire R, Nelson V, Rotimi O, Johnson R, et al. Pro-inflammatory TNFalpha and IL-1beta differentially regulate the inflammatory phenotype of brain microvascular endothelial cells. J Neuroinflamm. 2015;12:131.
102. Spittau B, Dokalis N, Prinz M. The role of TGFbeta signaling in microglia maturation and activation. Trends Immunol. 2020;41(9):836–48.
103. Lobo-Silva D, Carriche GM, Castro AG, Roque S, Saraiva M. Balancing the immune response in the brain: IL-10 and its regulation. J Neuroinflamm. 2016;13(1):297.
104. Lee J, Hwang YJ, Kim KY, Kowall NW, Ryu H. Epigenetic mechanisms of neurodegeneration in Huntington's disease. Neurotherapeutics. 2013;10(4):664–76.
105. Moumné L, Betuing S, Caboche J. Multiple aspects of gene dysregulation in Huntington's disease. Front Neurol. 2013;4:127.
106. Petkau TL, Hill A, Connolly C, Lu G, Wagner P, Kosior N, et al. Mutant huntingtin expression in microglia is neither required nor sufficient to cause the Huntington's disease-like phenotype in BACHD mice. Hum Mol Genet. 2019;28(10):1661–70.
107. O'Regan GC, Farag SH, Casey CS, Wood-Kaczmar A, Pocock JM, Tabrizi SJ, Andre R. Human Huntington's disease pluripotent stem cell-derived microglia develop normally but are abnormally hyper-reactive and release elevated levels of reactive oxygen species. J Neuroinflamm. 2021;18(1):94.
108. Rocha NP, Charron O, Latham LB, Colpo GD, Zanotti-Fregonara P, Yu M, et al. Microglia activation in basal ganglia is a late event in huntington disease pathophysiology. Neurol Neuroimmunol Neuroinflamm. 2021. https://doi.org/10.1212/NXI.0000000000000984.
109. Schilling G, Becher MW, Sharp AH, Jinnah HA, Duan K, Kotzuk JA, et al. Intranuclear inclusions and neuritic aggregates in transgenic mice expressing a mutant N-terminal fragment of huntingtin. Hum Mol Genet. 1999;8(3):397–407.
110. Hsiao HY, Chen YC, Chen HM, Tu PH, Chern Y. A critical role of astrocyte-mediated nuclear factor-kappaB-dependent inflammation in Huntington's disease. Hum Mol Genet. 2013;22(9):1826–42.
111. Posse de Chaves E, Sipione S. Sphingolipids and gangliosides of the nervous system in membrane function and dysfunction. FEBS Lett. 2010;584(9):1748–59.
112. Cutillo G, Saariaho AH, Meri S. Physiology of gangliosides and the role of antiganglioside antibodies in human diseases. Cell Mol Immunol. 2020;17(4):313–22.
113. Marth JD, Grewal PK. Mammalian glycosylation in immunity. Nat Rev Immunol. 2008;8(11):874–87.
114. Di Pardo A, Maglione V, Alpaugh M, Horkey M, Atwal RS, Sassone J, et al. Ganglioside GM1 induces phosphorylation of mutant huntingtin and restores normal motor behavior in Huntington disease mice. Proc Natl Acad Sci U S A. 2012;109(9):3528–33.
115. Maglione V, Marchi P, Di Pardo A, Lingrell S, Horkey M, Tidmarsh E, Sipione S. Impaired ganglioside metabolism in Huntington's disease and neuroprotective role of GM1. J Neurosci. 2010;30(11):4072–80.
116. Desplats PA, Denny CA, Kass KE, Gilmartin T, Head SR, Sutcliffe JG, et al. Glycolipid and ganglioside metabolism imbalances in Huntington's disease. Neurobiol Dis. 2007;27(3):265–77.
117. Shih RH, Wang CY, Yang CM. NF-kappaB signaling pathways in neurological inflammation: a mini review. Front Mol Neurosci. 2015;8:77.
118. Bachstetter AD, Van Eldik LJ. The p38 MAP kinase family as regulators of proinflammatory cytokine production in degenerative diseases of the CNS. Aging Dis. 2010;1(3):199–211.
119. Cuenda A, Rousseau S. p38 MAP-kinases pathway regulation, function and role in human diseases. Biochim Biophys Acta. 2007;1773(8):1358–75.
120. Carmody RJ, Chen YH. Nuclear factor-kappaB: activation and regulation during toll-like receptor signaling. Cell Mol Immunol. 2007;4(1):31–41.
121. Yan G, Huang J, Jarbadan NR, Jiang Y, Cheng H. Sequestration of NF-kappaB signaling complexes in lipid rafts contributes to repression of

NF-kappaB in T lymphocytes under hyperthermia stress. J Biol Chem. 2008;283(18):12489–500.
122. Kobayashi K, Hernandez LD, Galan JE, Janeway CA Jr, Medzhitov R, Flavell RA. IRAK-M is a negative regulator of Toll-like receptor signaling. Cell. 2002;110(2):191–202.
123. Escoll P, del Fresno C, Garcia L, Valles G, Lendinez MJ, Arnalich F, Lopez-Collazo E. Rapid up-regulation of IRAK-M expression following a second endotoxin challenge in human monocytes and in monocytes isolated from septic patients. Biochem Biophys Res Commun. 2003;311(2):465–72.
124. Lyn-Kew K, Rich E, Zeng X, Wen H, Kunkel SL, Newstead MW, et al. IRAK-M regulates chromatin remodeling in lung macrophages during experimental sepsis. PLoS ONE. 2010;5(6): e11145.

Publisher's Note